UNIVERSITÉ LIBRE DE BRUXELLES

Bruface
Brussels Faculty of Engineering

VRIJE UNIVERSITEIT BRUSSEL

Vehicle localization in underground tunnels using ultra-wideband ranging

Michael Gormez

Master thesis submitted under the supervision of
Prof. Dr. Ir. François Quitin

The co-supervision of
Dr. Ir. Michel Osée

In order to be awarded the Master's Degree in
Electrical Engineering

Academic year
2018-2019

Acknowledgements

I would like to thank my promoter François Quitin for all his guidance and regular checkups on my work and Michel Osée for his help with the logistics of the project. I would also like to thank Cédric Hannotier for helping me debug a particularly tedious part of the project. Next I would like to thank my family for letting me borrow their computers, cables and car to carry out some experiments. Finally I would like to thank my girlfriend Yorly Walteros for supporting me during the long nights working on our theses.

Michael Gormez

Abstract

This project presents the implementation of a Real Time Location System (RTLS) suited for indoor applications using Ultra-Wideband (UWB) ranging. It is implemented with the goal to use it to accurately track metro or train systems in underground tunnels, in this way allowing the operators to increase the frequency of their vehicles. The ranging method implemented in the RTLS is the Symmetric Double Sided Two Way Ranging(SDS-TWR) chosen for its ability to use a single antenna for each node involved in the ranging as well as not requiring synchronization between any nodes of the system. The trilateration algorithm implemented minimizes the Mean Square Error(MSE) and is more accurate when inside the triangle defined by the fixed anchors than outside. The results obtained show that the system is suitable for use in underground tunnels due to its resistance to multipath.

Keywords: RTLS,UWB,SDS-TWR,underground

Contents

Chapter 1

Introduction

1.1 Motivation

In recent years, the need for localization systems has been booming in very diverse fields. Localization is a valuable service that can help to localize its user or allows the user to localize objects of interest. Some applications are: providing a support to drone flight, helping to track assets in automatic factories or vehicle localization in general [1, 2].

Current localization systems rely largely on Global Navigation Satellite Systems (GNSS) technology, such as GPS, Galileo or Glonass. However, GNSS systems are unreliable in underground or indoor applications since the satellite signals cannot be received in these environments. This is a real problem for train and metro systems, for which an accurate localization of their vehicles would provide the possibility to increase the frequency of the vehicles [3].

Ultra-wideband (UWB) is an emerging wireless technology that allows to estimate the distance between two UWB sensors with centimeter-like accuracy. UWB doesn't suffer from the same unreliability in underground environment as GNSS since it doesn't depend on remote satellite communications to establish the position of an object, but rather on local UWB sensors [1, 3]. This accuracy and underground availability make UWB a suitable alternative to GNSS for this project.

1.2 Objectives

This project aims to implement an indoor Real Time Localization System (RTLS) working in underground tunnels. A mobile UWB sensor will be localized with regard to other fixed UWB sensors. The global objective for this RTLS is to provide an accurate localization of a train or a metro. This accurate localization can then be used by the operator to increase the frequency of its vehicles. To this end, the project has been separated in multiple parts, as highlighted below and reflected in the structure of the document.

ultra-wideband ranging

The first step of establishing the position of the mobile node is to choose a ranging method suited for UWB applications (chapter 2). This ranging method will be used to provide relative information about the position of the mobile sensor to a fixed sensor in the form of a Line Of Positions (LOP). The impact of different parameters of the inter-sensor communication on the ranging will be studied in chapter 4.

vehicle localization

Combining multiple ranging information, the absolute position of the vehicle can be computed using a localizing algorithm. Since a certain error is made on the measurement of the distance between two sensors, the goal of the algorithm is to minimize the absolute error on the estimated position using these imperfect information.
In a second phase, the position of the mobile sensor obtained will be updated over time during realistic experiments where the mobile node will be carried in a moving car.

underground tunnels

The underground nature of the communication brings information to the constraints on the communication channel. This should be used to assess which ranging method would be optimal, and how it impacts the range of the communication.

The timeline of the implementation realized to fulfill the project's objectives was the following:

- Configuring the SPI communication between the microcontroller (ESP8266, see [26]) and the UWB sensor (DWM1000, see [16]), where the μC is the SPI master and the sensor is the SPI slave. In the same vein, the configuration and tuning of the communication channel allowing the inter-sensor communication (setting center frequency, data rate, etc. see 2.5). Although this step was very tedious, it will only be scarcely presented in this document as it mainly consists in setting the appropriate bits in the appropriate registers of the DWM1000 to select the desired configuration (see annex C for a link to the complete code).

- Once the communication is functional, the ranging method can be implemented and calibrated ensuring its accuracy. It can then be tested under different conditions.

- Multiple rangings between one tag and multiple anchors were performed to obtain the absolute position of the tag by combining the ranging informations through the use of a localization algorithm.

Chapter 2

State Of The Art

2.1 Introduction

In this section, an overview of the state of the art of the different parts of this project will be presented. It will introduce the concept of RTLS and how its different parts can be implemented.It will conclude by comparing the different methods and motivate the choices made.

2.2 RTLS

A Real Time Locating System (RTLS) is a system used to provide information in Real-Time about the location of objects [17]. An RTLS can have many different architectures. However, indoor RTLS are generally composed by one or more mobile nodes, the *tags*, fixed nodes with a known position, the *anchors*, and an algorithm computing the absolute position of the tags with regard to the anchors[14].

The algorithm computing the absolute position of the tag can be decomposed in 3 parts:

1. The first part is to perform a ranging between a tag and a certain amount of anchors. This ranging provides information about the relative position between a tag and an anchor, such as a distance or an angle. Many ranging methods exist and are described in the next section.
2. In the second phase, the rangings obtained can be used to compute an absolute position of the tag with regard to the coordinate reference defined by the anchors.
3. The last function of the RTLS is to keep this absolute position updated over time.

This last point will be the object of a further chapter while the two first ones are presented here.

2.3 Ranging methods

The ranging method is the basis of the RTLS. Each ranging method has some advantages and some disadvantages. The objective of a ranging method is to obtain a Line of Positions

(LOP). A LOP is the set of positions where the ranging method determines that the tag can be situated. Multiple LOPs are needed to determine one absolute position of the tag.

When studying the different types of methods, it is important to keep in mind the particular field of application for this project. Indeed, underground environments come with important multipath components (MPC) since underground environments are restrained spaces with reinforced concrete surfaces. This will be investigated throughout the document.

In the following ranging methods, the tag will be noted T located at the unknown position $p_0 = (x_0, y_0)$ and the anchors will be noted A_i with positions $p_i = (x_i, y_i)$. The tag will be shown as red dots, while the anchor(s) will be shown as black dots.

$$Tag \quad T := p_0 = \begin{pmatrix} x_0 \\ y_0 \end{pmatrix} \tag{2.1}$$

$$Anchor \quad A_i := p_i = \begin{pmatrix} x_i \\ y_i \end{pmatrix} \tag{2.2}$$

2.3.1 RSS - Received signal strength

This method relies on measuring the strength of the measured signal. Based on this strength and the knowledge of the initial emitted power, the distance can be computed.

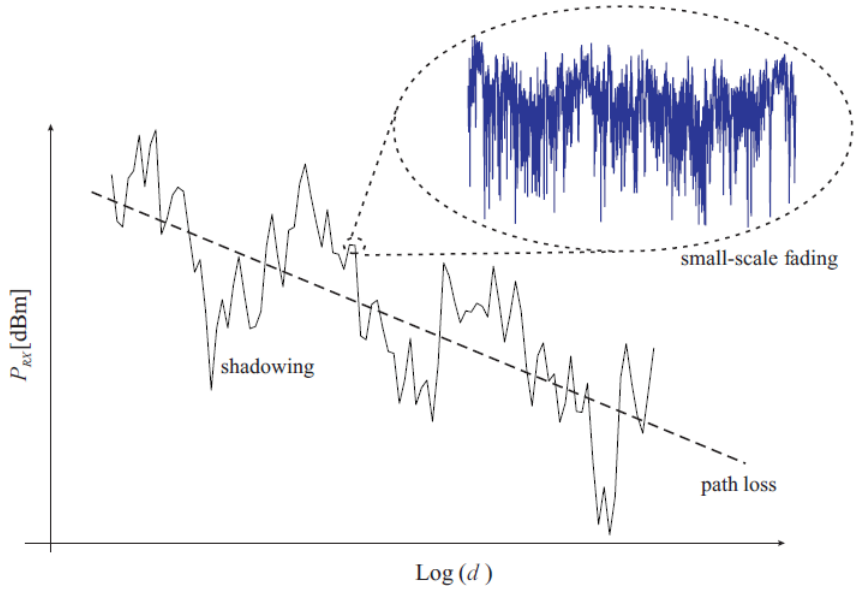

Figure 2.3.1: RSS - Received Signal Strength method[12]

However, as seen on the figure above, the RSS depends on multiple factors like path loss, shadowing and small-scale fading. A precise model of the channel taking into account these parameters due to interferences and due to the environment is not straight forward to obtain, leading to a poor accuracy. This is especially true in this context of underground localization.

2.3.2 AOA - Angle of arrival

AOA is based on measuring the angle of arrival between the direction of propagation of the signal and a reference direction.

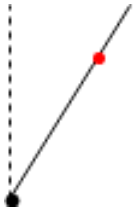

Figure 2.3.2: AOA - Angle of arrival

Each receiving element is composed of an array of antennas where each measures a slightly different TOA. From there, the direction of propagation of the signal can be computed. The LOP given by the angle information is a straight line. This means that from one AOA measurement, the tag is able to determine that its absolute position is somewhere on the LOP.
This ranging method is very sensitive to MPC, and the array of antennas required to measure multiple TOA make the system more expensive than other technologies.

2.3.3 TOA - Time of Arrival

To measure the TOA of a signal between a transmitter and a receiver, the duration of the signal and the speed of light can be used to recover a distance information.

Figure 2.3.3: Time of flight

$$TOF = (t_2 - t_1) \Rightarrow distance = TOF \cdot c$$

where TOF is the time of flight of the signal (duration to go from tag to anchor), c is the speed of light.
This method gives information about the distance between an anchor and a tag, and therefore its associated LOP is a circle. The equation of a circle is $(x - x_c)^2 + (y - y_c)^2 = r^2$

With 2.2, this can be rewritten to

$$(p - p_0)^T (p - p_0) = r_i^2 \tag{2.3}$$

where r_i is the distance measured between the tag (red) and the anchor (black).

The problem with this method is that for the timestamps to be usable, the mobile station and all the fixed anchors should be synchronized together.

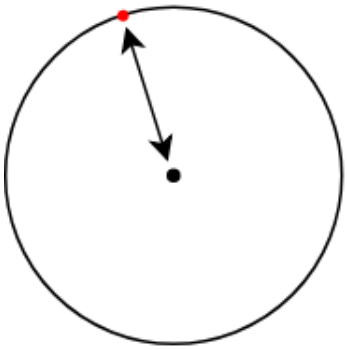

Figure 2.3.4: TOA LOP

2.3.4 TDOA - Time Difference of Arrival

TDOA measures the difference of TOA between a message sent from a tag B to fixed anchors P_1, P_2 and P_3. The difference between the time stamps of the 2 anchors is the useful information of this ranging. Therefore 2 anchor nodes are needed to perform a ranging instead of 1 anchor for the other methods.

The LOP obtained from a received time stamp pair is a hyperbola which has constant

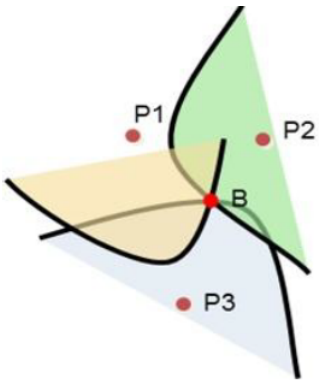

Figure 2.3.5: Time Difference Of Arrival

distance difference to the 2 anchors. This method requires synchronization of the anchors only (and not of the tag).

2.3.5 TWR - Two way ranging

In the TWR scheme, 2 messages are exchanged (instead of 1 for TOA). On the next figure, we can see that the TOF is given by

$$TOF = \frac{t_{roundA} - t_{replyB}}{2} \tag{2.4}$$

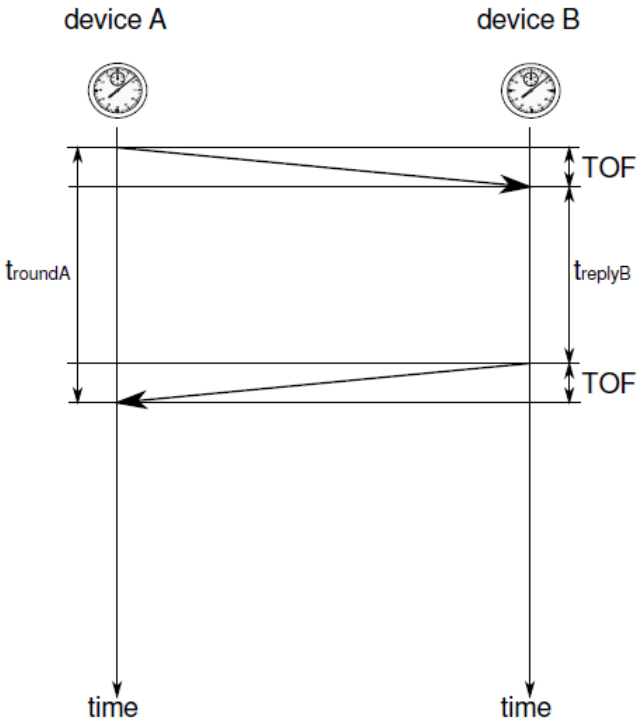

Figure 2.3.6: TWR [11]

However, if the clocks of the two devices do not tick at exactly the same frequency (clock drift), the following error is made.
By noting e_A and e_B the respective clock drifts, the TOF becomes

$$\widehat{TOF} = \frac{t_{roundA} \cdot (1 + e_A) - t_{replyB} \cdot (1 + e_B)}{2}$$

And the error due to the clock drift is the difference between TOF and $\widehat{TOF}$

$$\begin{aligned} & error = TOF - \widehat{TOF} \\ \iff & error = \frac{t_{roundA} - t_{replyB}}{2} - \frac{t_{roundA} \cdot (1 + e_A) - t_{replyB} \cdot (1 + e_B)}{2} \\ \iff & error = \frac{t_{replyB} \cdot e_B - t_{roundA} \cdot e_A}{2} \end{aligned}$$

By using equation 2.4 to express $t_{roundA} = 2 \cdot TOF + t_{replyB}$, we find the final expression of the error

$$\begin{aligned} & error = \frac{t_{replyB} \cdot e_B - (2 \cdot TOF + t_{replyB}) \cdot e_A}{2} \\ \iff & error = TOF \cdot e_A + \frac{1}{2} \cdot t_{replyB}(e_A - e_B) \\ \iff & error \approx \frac{1}{2} \cdot t_{replyB}(e_A - e_B) \end{aligned}$$

The error of this scheme is proportional the reply time. The next method will try to reduce this error.

2.3.6 SDS TWR - Symmetric Double Sided Two Way Ranging

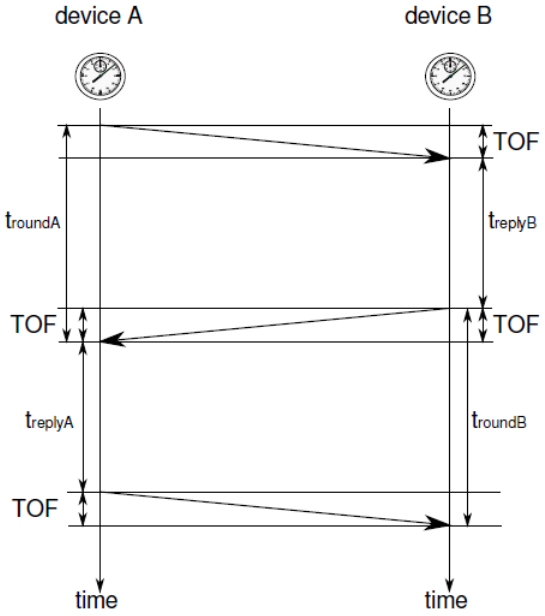

Figure 2.3.7: SDS TWR

The derivation of the error is very similar to the one for the TWR scheme. 2 TOF can be found in this scheme

$$2 \cdot TOF = t_{roundA} - t_{replyB}$$
$$2 \cdot TOF = t_{roundB} - t_{replyA}$$

and be combined in

$$4 \cdot TOF = (t_{roundA} - t_{replyB}) + (t_{roundB} - t_{replyA})$$

Taking the clock drift into account once again, this brings the estimated TOF to

$$\widehat{TOF} = \frac{(t_{roundA} - t_{replyA}) \cdot (1 + e_A) + (t_{roundB} - t_{replyB}) \cdot (1 + e_B)}{4}$$

The error made can be expressed as the correct TOF minus the measured $\widehat{TOF}$, affected by the clock drift

$$error = TOF - \widehat{TOF}$$
$$\iff error = \frac{(t_{roundA} - t_{replyA}) \cdot e_A + (t_{roundB} - t_{replyB}) \cdot e_B}{4}$$

We can then rewrite the reply times as

$$t_{replyA} = t_{reply}$$
$$t_{replyB} = t_{reply} + \Delta_{reply}$$

The round trip times then become

$$t_{roundA} = 2 \cdot TOF + t_{reply} + \Delta_{reply}$$
$$t_{roundB} = 2 \cdot TOF + t_{reply}$$

And the error $\widehat{TOF}$ - TOF is then given by

$$error = \frac{(2 \cdot TOF + t_{reply} + \Delta_{reply} - t_{reply})e_A + (2 \cdot TOF + t_{reply} - t_{reply} - \Delta_{reply})e_B}{4}$$
$$\iff error = \frac{1}{2} \cdot TOF(e_A + e_B) + \frac{1}{4}\Delta_{reply} \cdot (e_A - e_B)$$
$$\iff error \approx \frac{1}{4}\Delta_{reply}(e_A - e_B)$$

The error is now proportional to the difference in reply times. When using similar devices this Δ_{reply} is small and therefore the error is also small.

2.3.7 Conclusion

Symmetric Double Sided Two Way Ranging (SDS-TWR) emerges as the clear winner. It can benefit from UWB technology to decrease its sensibility to multipath (see 2.5) and also doesn't require any synchronization. Moreover, a single antenna per node is sufficient for this method which keeps the cost of the system down.

The bypassing of the synchronization step does come at the price that this method requires to exchange 3 messages to complete a single ranging (or 4 messages, depending on if we want to compute the position on the same device that initiates the communication).
UWB companies are split between using SDS-TWR and TDOA depending on the choice made for or against synchronization [1, 13, 14].

2.4 Positioning methods

A positioning method works by combining multiple LOPs to obtain a single absolute position in the referential of the anchor nodes.
Two main types of positioning methods exist, tied to the ranging method chosen:

- multilateration: uses LOPs carrying a distance information
- multiangulation: uses LOPs carrying an angle information

The LOP of the ranging method selected is a circle, and so the multilateration will find the intersection of the different LOPs obtained to determine the position of the tag. In 2D, 3

LOPs obtained from 3 different anchors are necessary for the mulitaleration to yield a unique solution for the position of the tag. In the case of 3 LOPs, multilateration can be called trilateration.

However, as with all measurements performed in the real world, a certain error is made on the measurements. Because of this the 3 LOPs might not intersect in a single point but rather define a region of confidence on the position of the tag.

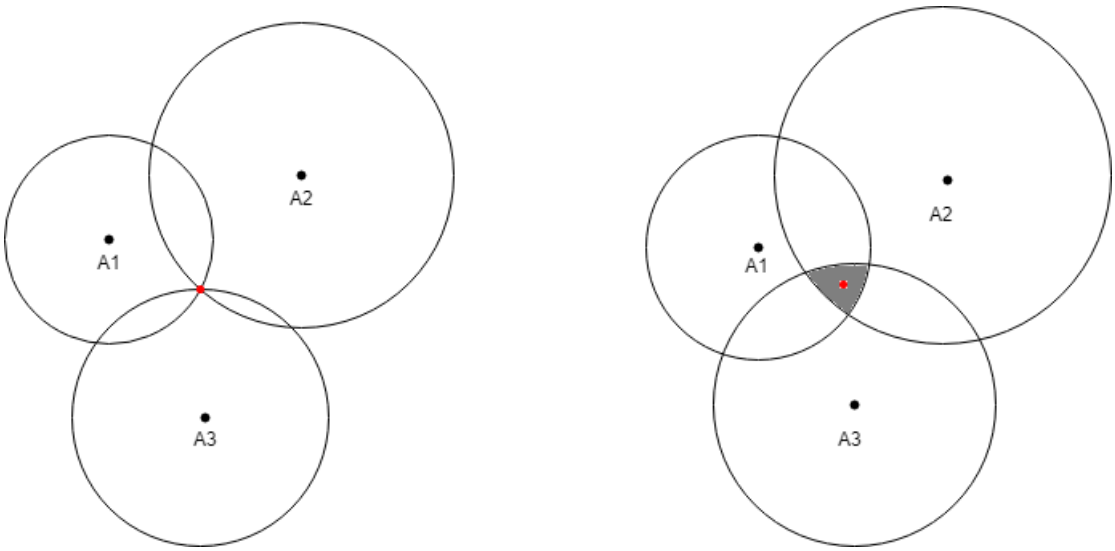

Figure 2.4.1: Trilateration without measurement errors (left) and with errors (right)

It is therefore necessary to explore a method allowing to extract an approximate position of the tag based on the imperfect measurements.

MSE

The method chosen to minimize this error is the Mean Square Error(MSE) minimization. Recalling equation 2.3, the MSE S minimizing the error of the absolute position of the tag p_0 is given by

$$S(p_0) = \sum_{i=1}^{N}((p_i - p_0)^T(p_i - p_0) - r_i^2)^2 \tag{2.5}$$

where N is the total number of anchors. In the 2D case, as shown on figure 2.4.1, 3 anchors are needed to localize the tag while in 3D 4 anchors are needed. The MSE aims to find an optimal tag position to minimize the MSE, that is a $p_{0,opt}$

$$p_{0,opt} = arg\min_{p_0} S(p_0) \tag{2.6}$$

To solve this problem, the algorithm proposed in [20] was implemented as an efficient trilateration algorithm. The algorithm is presented in annex D It takes as argument 3 distances issued by the rangings and outputs the optimal position for 2.6. The speed of the algorithm will be discussed in section 3.2 and the precision in chapters 4 and 5.

2.5 UWB

Definitions

Ultra-wideband (UWB) is a wireless technology used to transport high data rates at low power over a wide frequency range [25].A technology is categorized as UWB if at least one of the two following conditions are met:

- a bandwidth larger than 500 MHz is used
- a ratio of bandwith to center frequency (fractional bandwidth) of at least 20%

$$\frac{B}{f_{center}} \geqslant 20\%$$

UWB spectrum

The FCC authorizes UWB center frequencies between 3.1 and 10.6 GHz and an additional channel at 0.5GHz [5, 8, 9]. In that 7.5GHz band, the maximum output power for indoor applications is -41.3 dBm/MHz or 75 nW/MHz, which is considerably lower than other communication methods such as GPS Wi-Fi or Bluetooth.

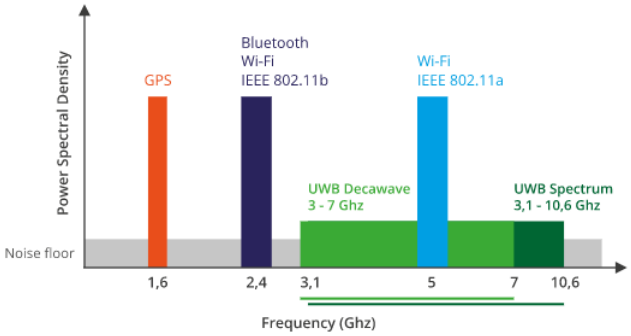

Figure 2.5.1: UWB spectrum

This low PSD makes UWB a particularly low energy form of communication, but also a low SNR. However this is not a problem for the channel capacity, which is given by the Shannon-Hartley theorem as

$$C = B \cdot log_2(1 + SNR)$$

The channel capacity C is indeed proportional to the Bandwidth B but only has a logarithmic dependency to the SNR, and UWB communications therefore have a large channel capacity available.

Band group[a] (decimal)	Channel number (decimal)	Center frequency, f_c (MHz)	Band width (MHz)	Mandatory/Optional
0	0	499.2	499.2	Mandatory below 1 GHz
1	1	3494.4	499.2	Optional
	2	3993.6	499.2	Optional
	3	4492.8	499.2	Mandatory in low band
	4	3993.6	1331.2	Optional
2	5	6489.6	499.2	Optional
	6	6988.8	499.2	Optional
	7	6489.6	1081.6	Optional
	8	7488.0	499.2	Optional
	9	7987.2	499.2	Mandatory in high band
	10	8486.4	499.2	Optional
	11	7987.2	1331.2	Optional
	12	8985.6	499.2	Optional
	13	9484.8	499.2	Optional
	14	9984.0	499.2	Optional
	15	9484.8	1354.97	Optional

[a]Note that bands indicate a sequence of adjacent UWB center frequencies: band 0 is the sub-gigahertz channel, band 1 has the low-band UWB channels, and band 2 has the high-band channels.

Figure 2.5.2: UWB frequency bands defined in IEEE802.15.4-2011 [9]

UWB pulse

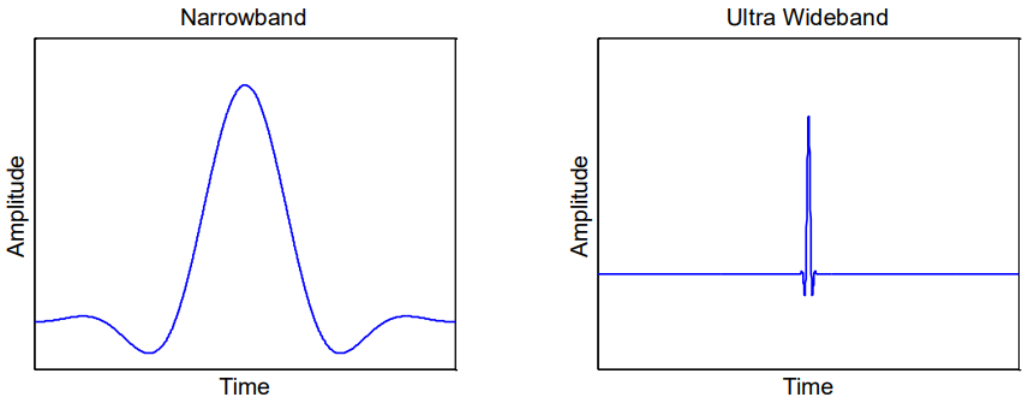

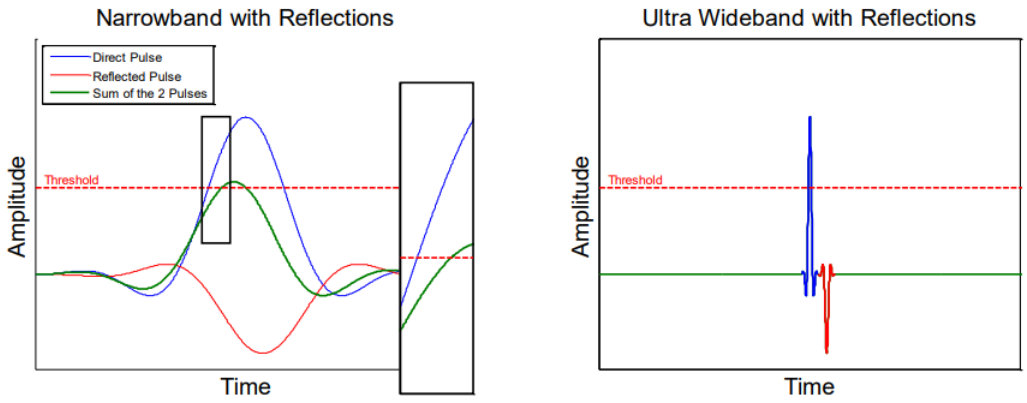

Figure 2.5.3: UWB pulse in time domain [6]

The main property of UWB is its very short pulse. Indeed, since the bandwidth used is very large, the time-domain pulse is very narrow with pulse length τ

$$\tau = \frac{1}{B}$$

For B of 500 MHz, this would translate to a pulse width of $\tau = 2ns$.
This short pulse is very useful as in this way it allows UWB based technologies to be resistant to multipath as well as supporting high data rates.

DWM1000

The DWM1000 sensor used in this project supports 6 frequency bands between 3.5 to 6.5 GHz, bands 1,2,3,4,5 and 7 [16]. It supports data rates of 110 kbps, 850 kbps and 6.8 Mbps and bandwidth up to 900 MHz, which means that channels and 4 and 7 will use a smaller bandwidth than allocated in the standard.

The *default channel configuration* also called standard conditions in this document, used in the DWM1000 is defined as being: channel 5, preamble code 4, preamble length 2048 symbols, 16 MHz PRF, data rate 6.8Mbps.

The DWM1000 provides 63 registers of variable size. These registers can be used for either setting the parameters of the communication (channel, preamble code, preamble size, etc.) or for reading the data and timestamps associated with the message exchange in the ranging. The complete datasheet is available in [16]. The configuration process necessary for this project is summarized in Annex C.

The DWM1000 is widely used in commercial UWB localization systems [13, 14, 15]. For indoor applications, the expected maximum range is from 10m to 30m depending on the configuration, with an error of the order of a dm.

2.6 Conclusion

In this chapter we have presented the concept of RTLS and reviewed different ranging methods and justified the choice of the Symmetric Double Sided Two Way Ranging (SDS-TWR). We have then explained the need for a localization algorithm that stems from the inherent measurement errors of the distance between the tag and the anchors. Finally we have shown the interesting properties in UWB, in particular its resilience to multipath due to its narrow time-domain pulse.

Chapter 3

Setup and calibration

This chapter will open by briefly reviewing the hardware used to support the ranging and will follow by presenting the program flow that was implemented from the different ranging steps to the computation of the absolute position. This will be followed by an mandatory calibration, which will allow to conclude the chapter by attempting to measure the maximum range of the system and to take a first look at the presence of MPC in underground tunnels.

3.1 Node structure

Each node is composed of a microcontroller ESP8266 [26] connected to an UWB sensor DWM1000 [16].

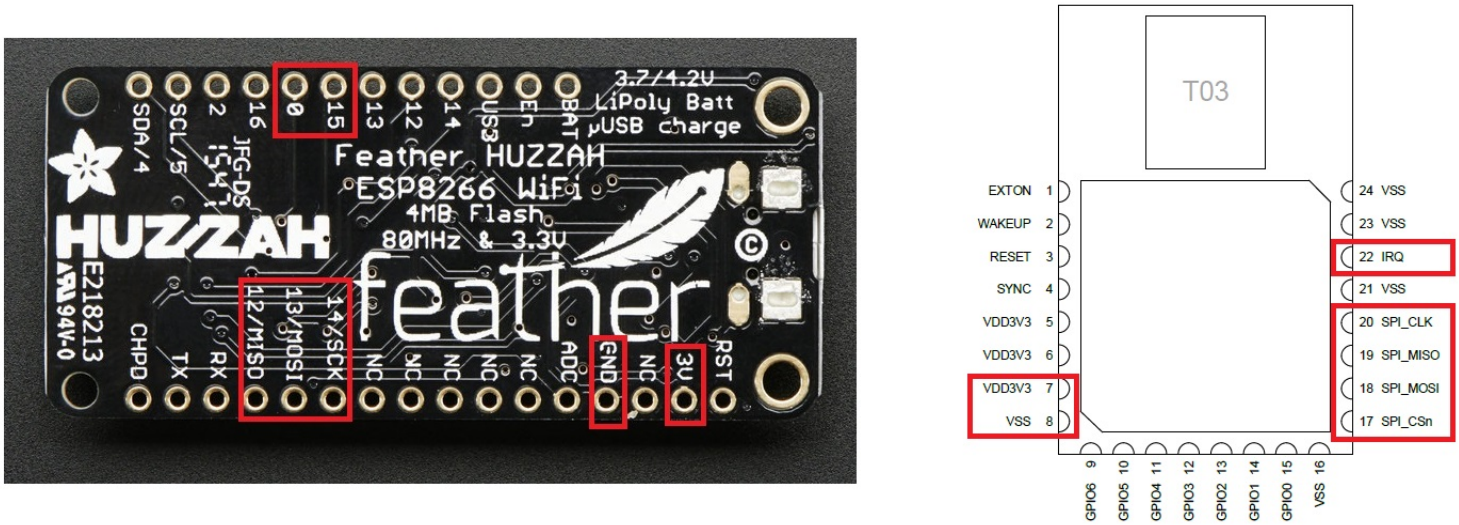

Figure 3.1.1: DWM100 and ESP8266 pinout

The pins are connected according to the next table.

pin function	esp8266	dwm1000
V_{DD}	3V	VDD3v3(7)
V_{SS}	GND	VSS(8)
spi clock	SCK(14)	SPI_CLK(20)
spi mosi	MOSI(13)	SPI_MOSI(18)
spi miso	MISO(12)	SPI_MISO(19)
spi chip select	(15)	SPI_CSn(17)
interrupt	(0)	IRQ(22)

Table 3.1: Pin connections

Each μC communicates by SPI with its sensor, where the μC is the SPI master and the sensor its SPI slave. Each μC has a micro USB port to connect it to the computer which serves both as a power supply and as a way to upload the program. The communication between two nodes is ensured by their respective DWM1000 sensors once the communication channel parameters have been selected according to section 2.5.

The localization setup is composed of 2 types of nodes. Mobile station nodes[1] (the *tags*) and fixed stations nodes (the *anchors*). The localization setup will cover how these can be used to perform localization.

In this section, we will first present the structure of the different components used for the localization and then describe the algorithm supporting it.

3.2 Program flow

The program is written in C++ and the toolchain used to flash the memory of the μC is arduino (see annex B). The program flow for the tag is shown on Fig 3.2.1 on the next page. The program flow of the anchors is similar to the one of the tag, except that no distances or position are computed.

After the one time initialization step is performed, the tag initiates the ranging with each anchor one by one[2]. After a ranging is done, the tag computes the distance and starts the next ranging. Once 3 rangings have been performed, the tag can use the localization algorithm to compute its absolute position in the referential defined by the fixed anchors.

[1] Although only 1 mobile node was used in this project, multiple nodes could be used if they have been properly synchronized to not send messages simultaneously (TDMA for example)

[2] the message sent by the tag contains an anchorID number which the anchors use to determine to which anchor the message is addressed

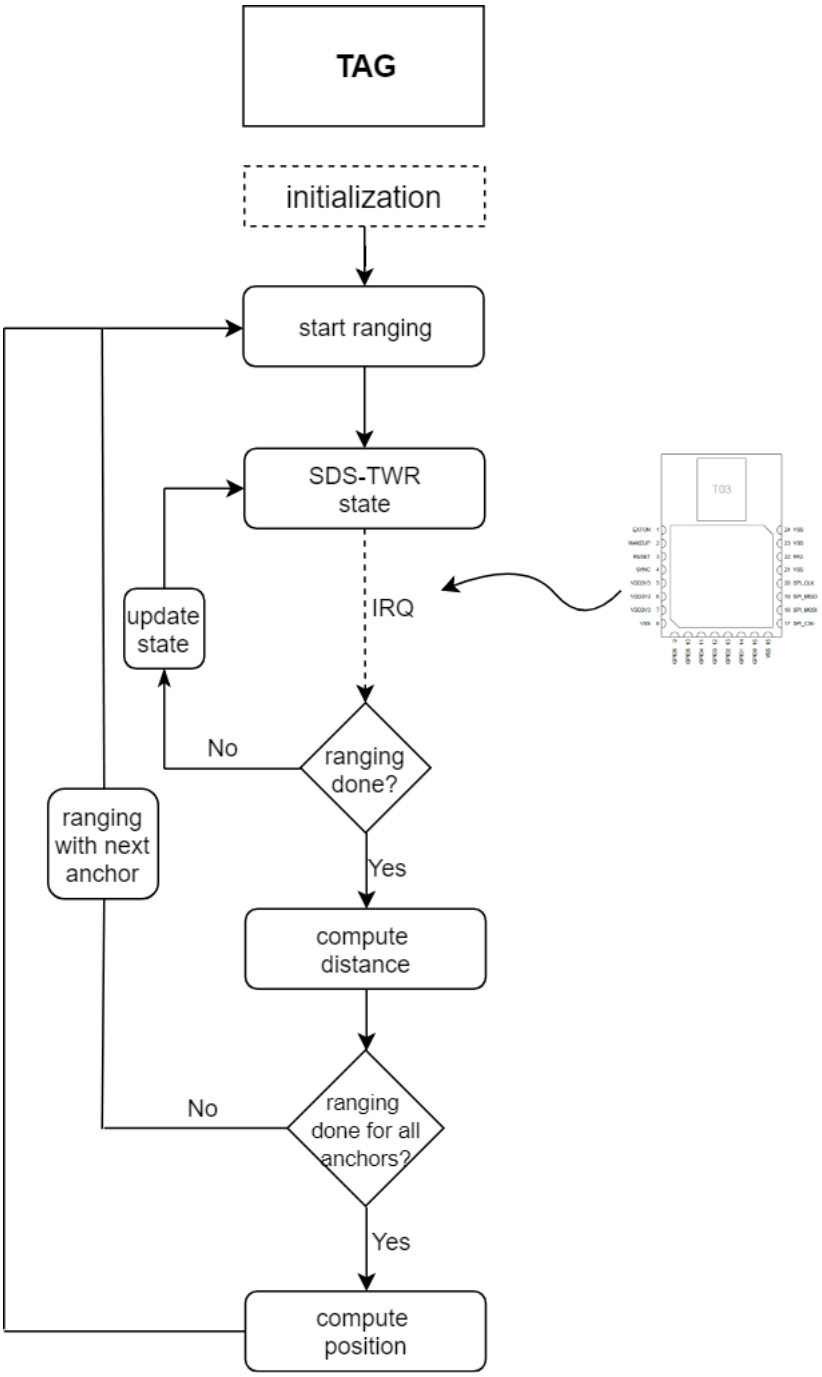

Figure 3.2.1: Program flow of the tag

The message exchange (which is detailed next) is based on interrupts. When a sensor completes a transmission or a reception, it triggers its interrupt line and the μC executes the interrupt service routine. The μC reads the status register of the sensor which contains information about the nature of the interrupt that was triggered. The tag then checks which state of the ranging it is in, in order to either continue the ranging, compute the distance with the current anchor or compute the position if all the rangings are done.
If no emission/reception occurs during a certain timeout period (set to 500ms), the tag de-

termines that a problem occured and the ranging restarts from scratch.

Ranging algorithm

The ranging algorithm implementation is explicited next. Blue and red states mean that the node is respectively in receive or transmit mode.

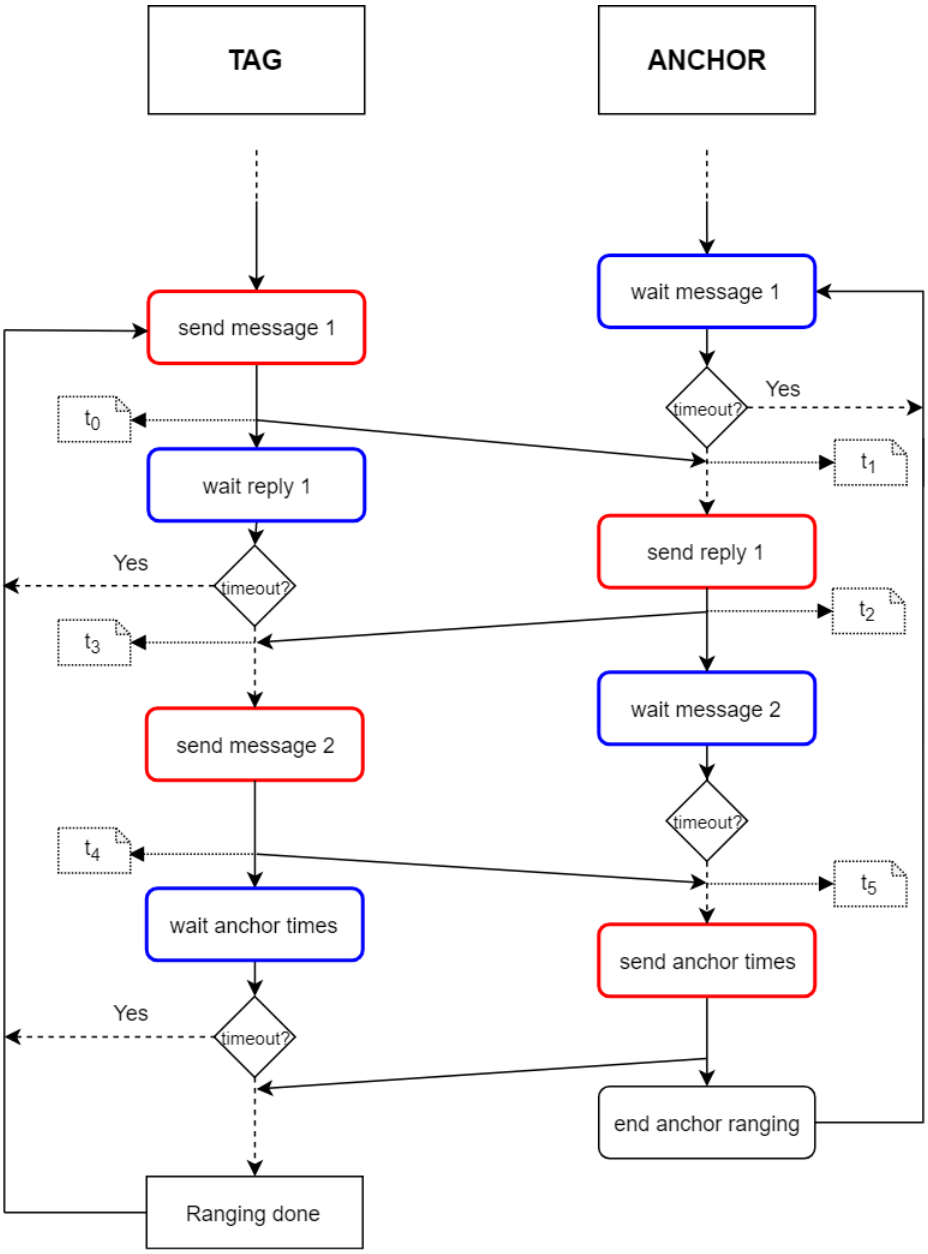

Figure 3.2.2: Ranging algorithm

The message exchange supporting the ranging is decomposed into the following steps

1. The tag prepares the message for the current anchor by embedding the anchorID in the message

2. Once the tag sends the message, it triggers an interrupt and saves the time of emission (t_0) that is then recorded by its μC
3. All anchors receive the message and trigger an interrupt. The μC of the anchor then determines if the message was destined to it by using the anchorID, and only the correct anchor of destination saves the time stamp of the reception (t_1).
4. Steps 1. through 3. are then performed again with reversed roles for the anchor and the tag to obtain t_3, t_4 and t_5.
5. Finally, the anchor sends the timestamps it recorded (t_1, t_2 and t_5) to the tag which concludes the ranging and allows the tag to compute its distance to the current anchor

Performance analysis

To conclude the presentation of the software implementation of the different elements of the project, it is interesting to conduct a time-performance analysis of the complete program. In this way, we will measure the time taken by the message exchange, the distance computation and the position computation. The configuration of the sensors will not be analyzed as it is a one-time operation taking place before any ranging.
The time-budget is split as follows:

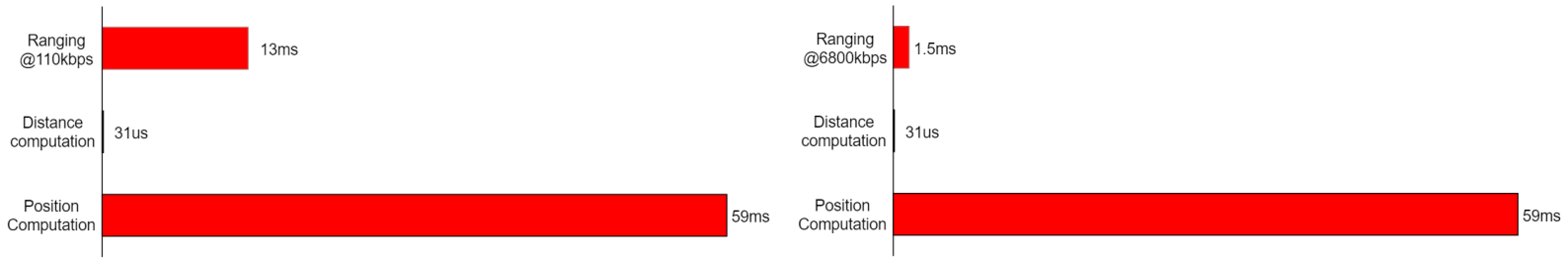

Figure 3.2.3: Algorithm performance

where the ranging time is the sum of the times of all the required message exchanges. For a 110kbps data rate, the total computation of a positioning is 72ms while it is just over 60ms for the 6800kbps. The bottleneck of the positioning is the computation of the position using the pre-computed distance information. The timings are summarized below.

- ranging@110kbps: 13.896 ms
- ranging@6.8Mbps: 1.576 ms
- distance computation: 31 μs
- position computation: 59 ms

3.3 Calibration

Before being able to perform a localization, a calibrating step of the rangings is needed. It will consist in comparing the output data of the ranging algorithm to a reference distance measured with other means in order to calibrate the antennas of the sensors. This serves to correct for the delay induced by the duration of the processing of each frame.

On the next figure, we can see the raw distance (without taking the antenna delay into account) resulting from the ranging previously described.

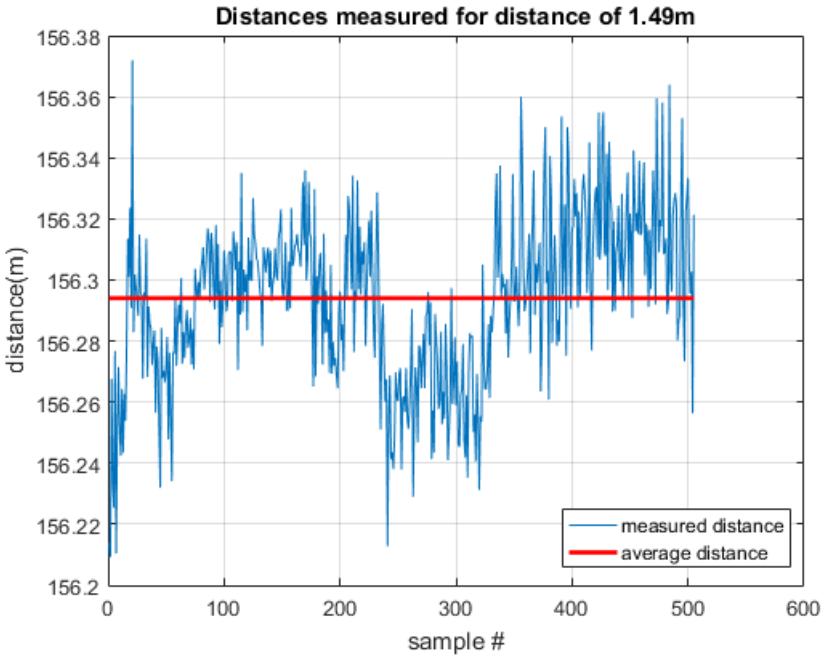

Figure 3.3.1: Uncalibrated ranging

The mean value of these measurements is 156.294 m while the real distance was of 1.49m which is a *quite* significant difference. This is due to an incorrect placement of the timestamp due to the overhead time needed for processing a frame, which corresponds to the offset induced by the antenna delay. To correct this, a first ranging is performed without taking the antenna delay into account and the antenna delay is adjusted based on the difference between the real distance value and the measured value. In this example, we have:

$$\begin{aligned} real\_distance &= 1.49m \\ average\_measured\_distance &= 156.294m \\ \Rightarrow average\_error &= 154.804m \end{aligned}$$

From this average error, we can find the offset to correct the timestamp with. Knowing the propagation speed of the messages, the speed of light $c = 299792458m/s$, and the error on the distance, we can compute the time error corresponding to the distance error

$$v = \frac{d}{t} \iff t = \frac{d}{v} = \frac{average\_error}{c} = \frac{154.804}{299792458} = 516.37ns$$

IEEE 802.15.4-2011 standard defines a sampling clock associated with the ranging with frequency 64GHz[1]. This corresponds to a period (and therefore a precision) of 15.65 ps, which translates to an equivalent distance-precision of 4.7mm.

$$distance\_resolution = \frac{c}{f} = \frac{299792458}{64 \cdot 10^9} = 4.7mm$$

$$antenna\_delay = \frac{t}{clock\_period} = \frac{516.37ns}{15.65ps} = 32995$$

This 32995 value represents the number of clock periods of the 64GHz clock needed to correct the delay of due to the processing of the frame. This delay can either be added at both the receiver and the transmitter, or an aggregate value can be added on one side only (of 65990). After some fine tuning, the aggregate value added on the anchor side was corrected to 65767. Taking this delay into account and restarting the ranging procedure, we obtain the following corrected measurements:

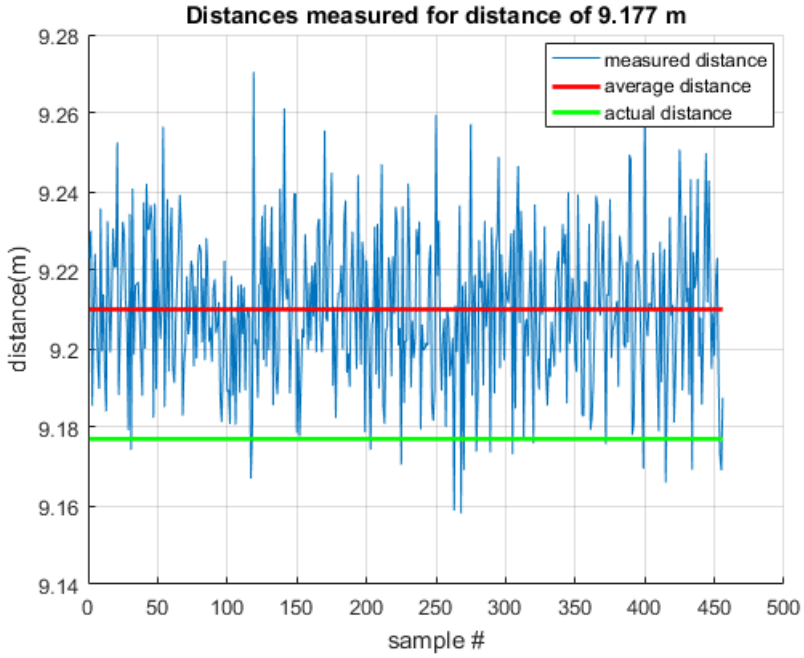

Figure 3.3.2: Calibrated ranging

Finally, it is important to note that the distance offset to be corrected doesn't vary greatly with the distance, and therefore a same antenna delay can be kept regardless of distance, which is important in a localization application where the distance between the tag and the anchors varies continuously.

[1]The exact frequency is $f = 128 \cdot 499.2 \cdot 10^6 Hz \approx 63.8976 GHz$

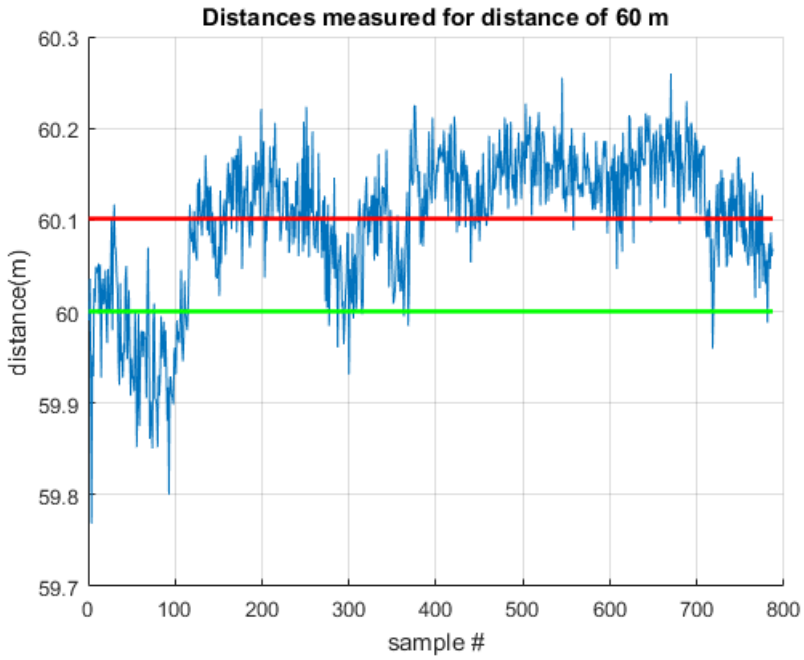

Figure 3.3.3: Calibrated ranging

The error is slightly higher (about 10cm), but there is some incertitude about the real distance. Indeed, a 10m meter and a Fluke [19] were used to measure the real distance as accurately as possible but a measurement error for measuring 60m is to be expected.

- error between real and estimated distance: 0.1m
- max error: 0.2598m

3.4 Maximum distance

Now that the accuracy of the ranging method has been verified, it is interesting to find the range over which it can be used. This section will serve this purpose and will also introduce the notion of probability of connection used further in the document.

Outdoor measurements

Although this first measurement was performed outside, it proved to be a valuable tool to try and troubleshoot the indoor measurements. It was carried out by simply leaving an anchor node on a chair and walking at a constant speed with the tag node.

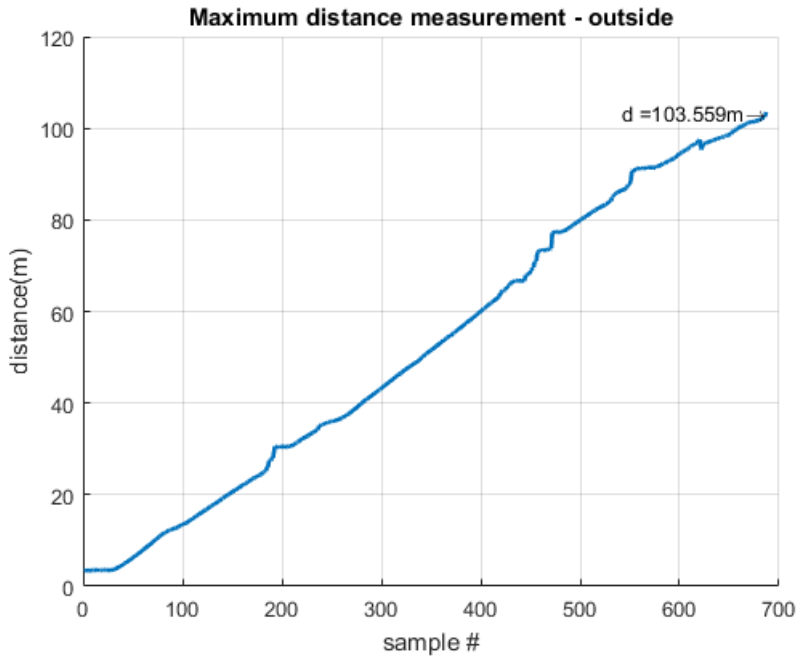

Figure 3.4.1: Maximum distance in outdoor standard conditions

A measurement performed in similar conditions with a datarate of 110kbps yielded a slightly higher distance (109m) but nothing conclusive.

The *probability of connection* for this experience is 90.27 %. The probability of connection has been defined as the number of good *complete rangings* over the total amount of rangings attempted. An error occurs when the ranging times out (see section 3.2).

$$P_{connection} = \frac{good\ rangings}{total\ ranging\ attempts}$$

where the total ranging attempts is the number of good rangings summed with the number of unsuccesful rangings (time outs).
The emphasize is put on the successful complete rangings and not message transmissions. Since 4 consecutive messages need to be successfully exchanged to make one ranging, the actual amount of correctly transmitted messages is always higher than the probability of connection.

Since this measurement was very successful (it attained a high range reliably) and that outdoor applications are not the focus of this project, no other measurements were carried out outdoors.

Indoor measurements

The first test performed indoor was to reproduce the outdoor measurement. As little material was available on the first day of measurements, the anchor node was sitting on the floor while the tag node was carried around by hand.

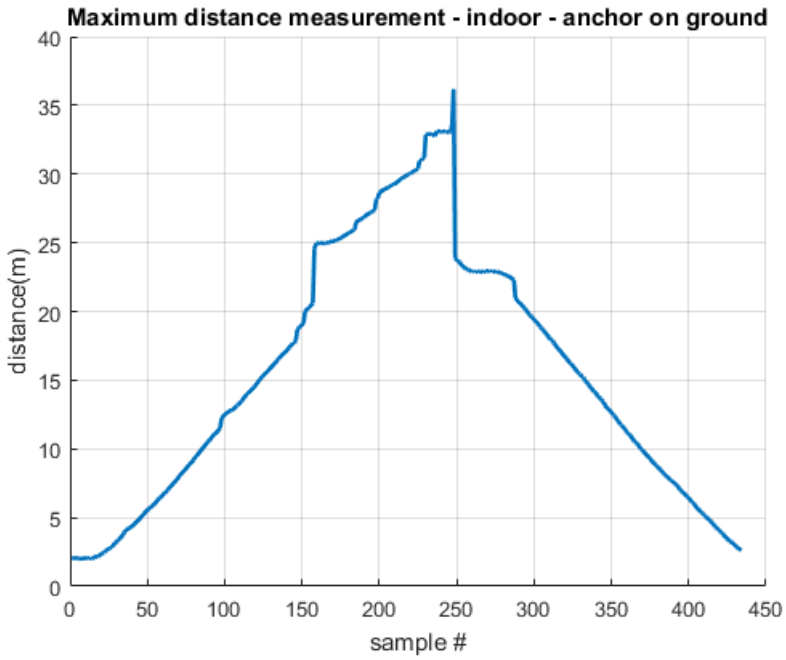

Figure 3.4.2: Maximum distance in indoor standard conditions

This time the results are unsatisfying and unexpected considering the outside measurement carried out. The range dropped to around 35m with a probability of connection of 68%. However, the probability of connection is above 95% for distances under 20m but only around 30% when above this distance threshold. A second test was then performed by lowering the data rate to 110kbps.

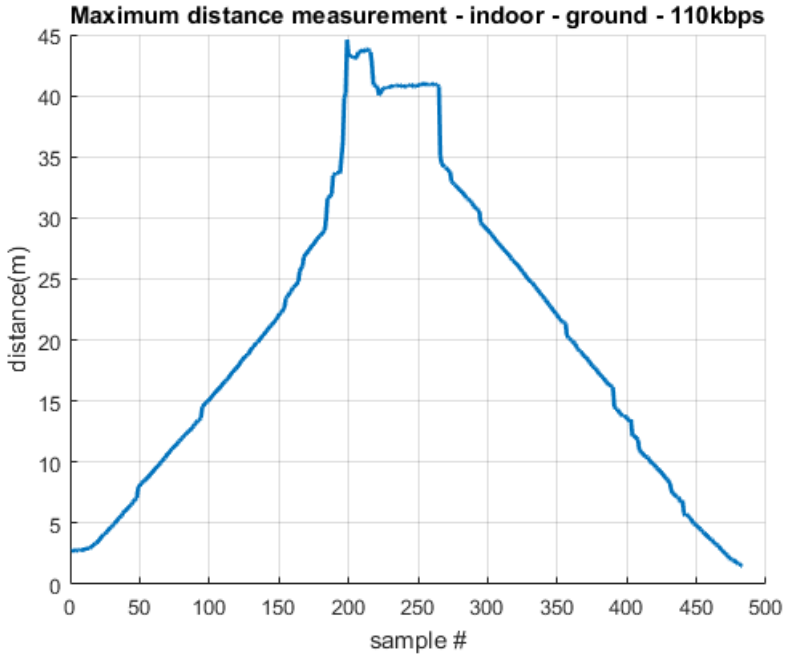

Figure 3.4.3: Maximum distance in indoor standard conditions

The improvement is immediate, this second measurement giving a range of above 40m and a probability of connection of 60% overall and 90% until 40m.
An alternative to changing the data rate is to elevate the anchor at a certain height (coming back to the initial 6800kbps), in this case about 1.6m from the ground.

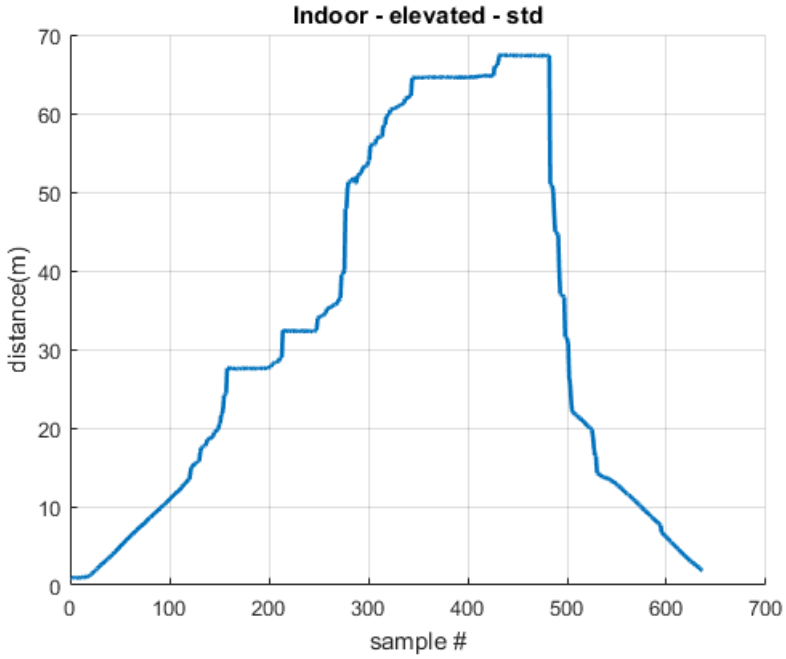

Figure 3.4.4: std condtions

This test emphasized the importance of having clearance from the ground (or from an obstacle in general) bringing the range to 70m[1] and and a probability of connection of 80%.

A last test was then performed combining the lower data rate of 110kbps with the anchor elevated of 1.6m from the ground.

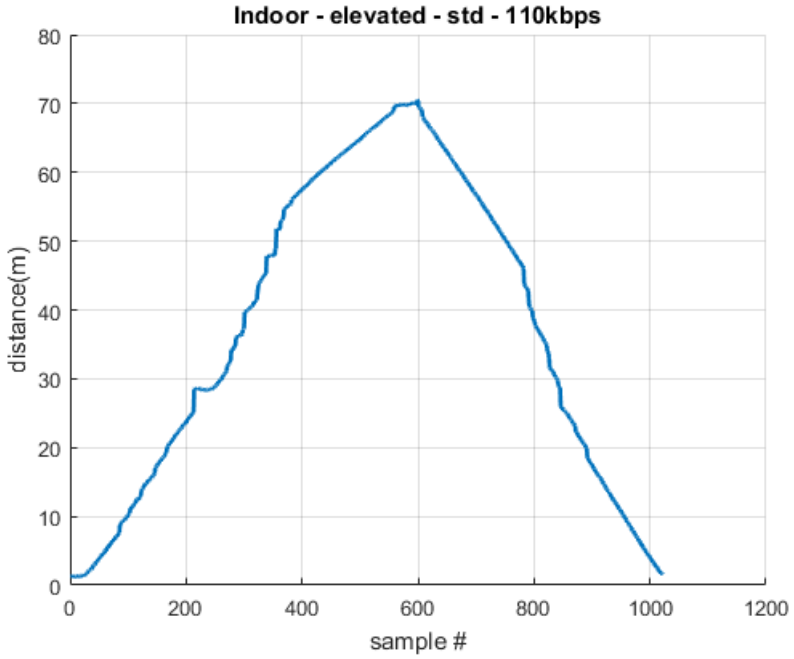

Figure 3.4.5: std conditions @110kbps

The range obtained is at least 70m with a connection probability of 85%. These measuring conditions (elevated anchor, standard channel configuration with data rate of 110kbps) will be used in the rest of the project unless stated otherwise.

3.5 Multipath

UWB technology is robust to multipath as presented in section 2.5, and multipath is very present in underground environments. This multipath presence will be illustrated in the last experience which will close this section.

The following measurements were obtained by blocking the line of sight(LOS) component by placing an anchor on one side of a column and the tag on the other side (see figure 4.1.1 for a global view of the parking). Since no communication is supposed to take place(because we know that the column is capable of blocking the LOS), if a ranging still takes place we know that a multipath component(MPC) is present and received.

[1]70m was the maximum indoor distance available during the experiments, so the maximum range is at least this distance

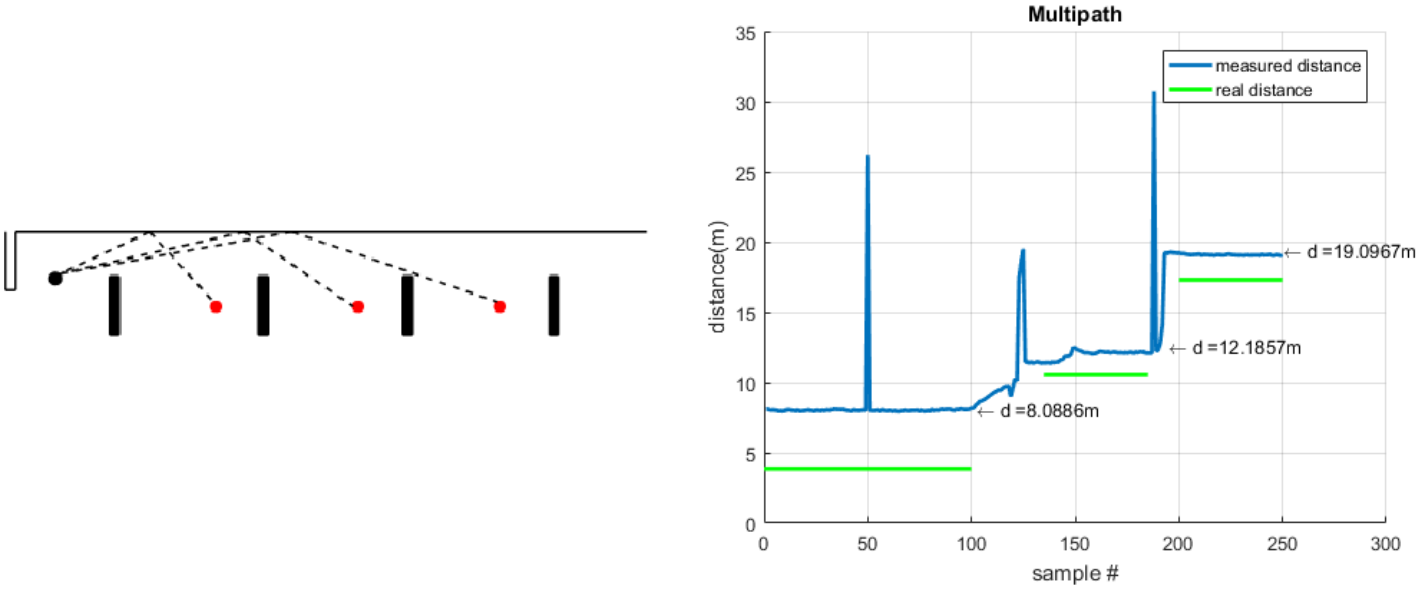

Figure 3.5.1: Multipath

As expected, multipath components are picked up and even allow a ranging for up to 20m. We can also see spikes in the measurements which must be due to another multipath component reflected from the opposite wall.

This experiment highlighted 2 important phenomenons.

1. Multipath components are present and have a strong intensity: they would allow a ranging over a distance of 20m by themselves which is around 20% of the ranging ability of the system.

2. The difference between the measured distance of the multipath component and the real distance decreases with distance.
   In the following table, the errors are related to the error between the measured (MPC) distance and the real distance.

real distance(m)	measured distance(m)	error(m)	error(%)
3.86	8.09	4.23	109.6
10.57	12.19	1.62	15.3
18	19.10	1.1	6.1

Table 3.2: Multipath evolution

As the distance between anchor and tag increases, the multipath component gets closer to the LOS component (would he have been present). This is problematic because as the distance increases, the interference between the two components increases. Although the interference increases the received power, this doesn't improve the quality of the ranging in our implication.

In the multipath measurement performed only one (or rarely two) multipath component was present and its origin was known. However in the more complex measurements performed in other scenarios, this is not the case

3.6 Conclusion

In this section, the choice of operating channel parameters has been fixed to channel 5 (center frequency of 6.5 GHz and bandwidth of 500MHz), preamble code 4, preamble length 2048 symbols, PRF 16MHz, data rate of 110 kbps. This configuration will be reused throughout the document as the standard configuration at 110kbps.

This configuration proved to have a range sufficient enough to perform at more than 85 % connection probability at the longest available underground distance in these experiments (70m). The anchor and tag nodes should additionally be cleared from the ground or the walls, which is why they were elevated of about 1.6m. This elevation will also come in handy when performing measurements in the car in chapter 5 as the metal body of the car was found to block the LOS component as well. Following that, the strong presence of MPC has been confirmed.

Chapter 4

Localization

4.1 Introduction

This chapter will build on the results established in the previous chapter. In this chapter the tag will perform rangings with multiple anchors in order for the tag to position itself using the algorithm already introduced in section 2.4. Different configurations will be tried out to see their effect on the localization.

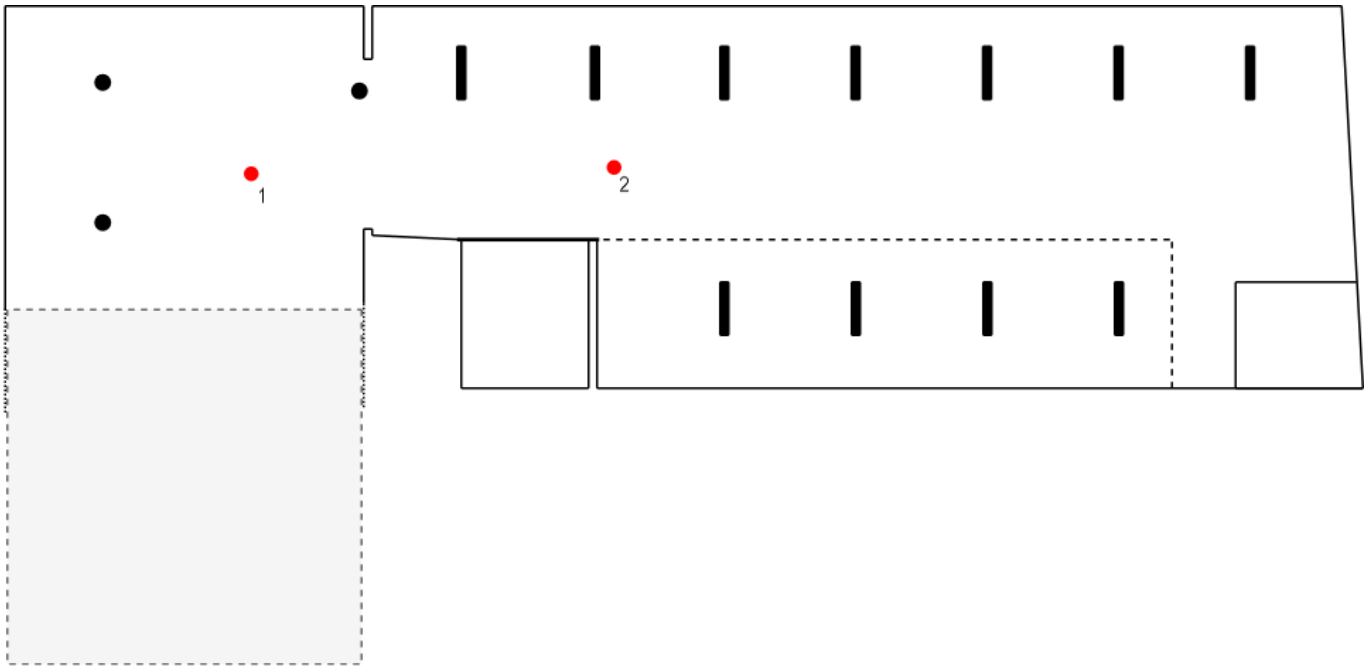

Figure 4.1.1: Parking geometry (top view)

The geometry of the parking where the tests were performed (lowest parking level of the parking in building S) is sketched on the figure above. The grey area is an elevated area leading to a higher parking level with an elevation rate of around 10°.
The first figure shows the top view where the black elements are the columns distant from each other of 6.25m and made of concrete blocks of section 1.2m by 0.34m up to the ceiling.

The distance between the columns and the outer walls is 2m. The dashed line represents a metal fence with a very thin grid.
The 3 black dots represent a typical anchor configuration used to perform tests. The first red dot (with index 1) represents the first position of the tag and the other represents the second.
The ceiling of the parking is quite low, with supporting beams sitting just 2.2m above the floor and situated on the same lines than the columns.

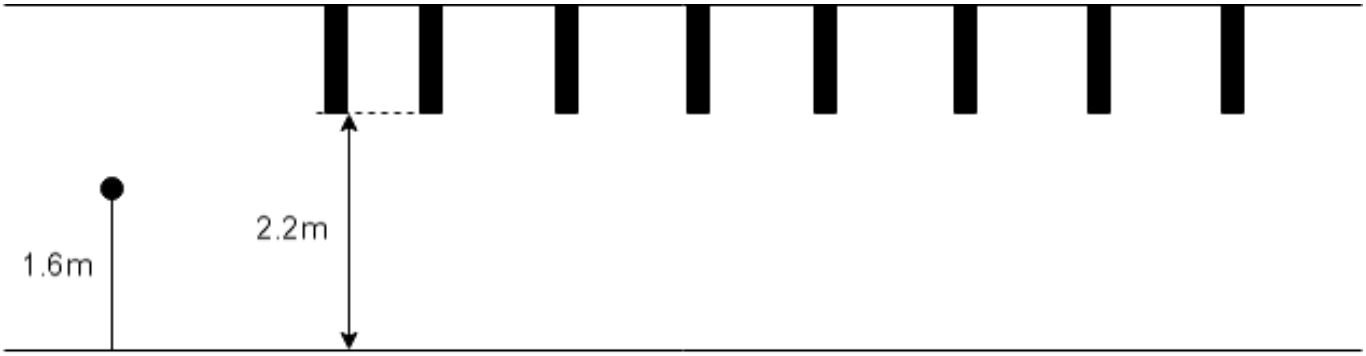

Figure 4.1.2: Parking geometry(lateral view)

The geometry of the parking will help to understand where MPCs could appear.
As justified in the previous chapter, the anchors are cleared from the ground by standing on a camera base. The tag will be cleared from the ground as well, either by being placed on a camera base similarly to the anchors or by being carried above a car during the tests involving movement of the tag, at the same height than the anchors.

4.2 Multipath interference

In the previous chapter the presence of MPC has been established. It is now interesting to study how these MPC could interfere with the LOS signal.
The signal emitted from the tag (and the replies of the anchor) have this general shape.

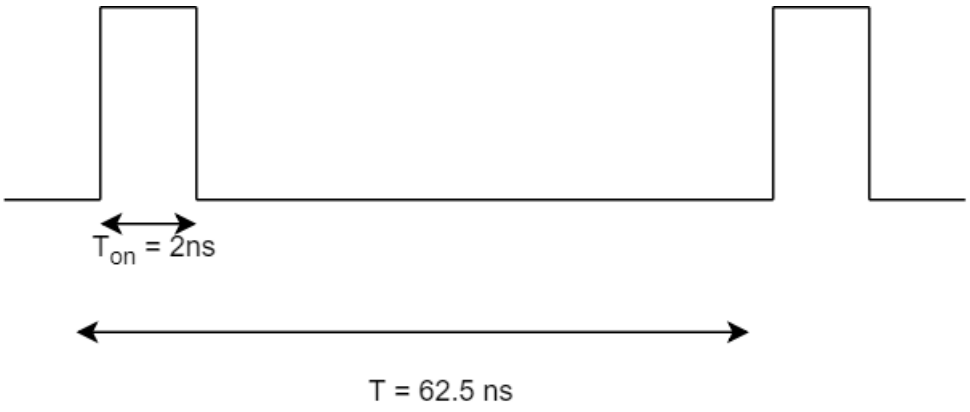

Figure 4.2.1: Signal shape, PRF = 16MHz, B = 500MHz

The T time is dictated by the selected PRF while the T_{on} time is dictated by the bandwidth. Values for these 2 parameters are summarized hereafter.

PRF(MHz)	B(MHz)	T_{on}(ns)	T(ns)	$d_{resolution}$(m)
16	/	/	62.5	18.75
64	/	/	15.625	4.6875
/	500	2	/	0.6
/	900	1.11	/	0.33

Table 4.1: distance resolution in function of PRF and bandwidth

The periods T and on-periods T_{on} are respectively equal to $\frac{1}{PRF}$ and $\frac{1}{B}$.
The distance resolution is the distance associated to this time, illustrated below for the 500MHz bandwidth with characteristic time t = 2ns

$$\begin{aligned} d &= c \cdot t \\ \Rightarrow d &= 3 \cdot 10^8 \cdot 2 \cdot 10^{-9} \\ &= 0.6\, m \end{aligned}$$

In this example, if we find a MPC of length *smaller* than the LOS length + 0.6m, this MPC will interfere with the LOS component. For the distance resolution associated to the PRF, if there is a MPC of length equal to *a multiple of* the distance resolution[1], a transmitted symbol can interfere with a next transmitted symbol. From this interpretation, we can also see that the 64 MHz PRF and the 500MHz bandwidth will be more sensitive to multipath since their resolutions are worse.
Although the distance resolutions associated to the PRF are large, in underground tunnels such MPCs could exist but will however not be a factor in this project.

The first configuration (channel 5, 16MHz PRF, 500MHz bandwidth) will be sensitive to MPC that have a length differing of less than 0.6m from the LOS component, and also to MPC differing from the LOS component by 18.75m $\pm$ 0.6m.

The over the ground MPC's length will interfere with the LOS component when $d_{NLOS} < d_{LOS}$+0.6m, that is for a LOS distance of

$$\begin{aligned} & d_{NLOS} = 2 \cdot \sqrt{(\frac{d_{LOS}}{2})^2 + h^2} \\ \iff & d_{LOS} + d_{resol} = 2 \cdot \sqrt{(\frac{d_{LOS}}{2})^2 + h^2} \\ \iff & d_{LOS}^2 + d_{resol}^2 + 2 \cdot d_{resol} \cdot d_{LOS} = 4 \cdot \frac{d_{LOS}^2}{4} + 4 \cdot h^2 \\ \iff & d_{resol}^2 + 2 \cdot d_{resol} \cdot d_{LOS} = 4 \cdot h^2 \\ \iff & d_{LOS} = \frac{4 \cdot h^2 - d_{resol}^2}{2 \cdot d_{resol}} \end{aligned}$$

[1]With a precision of the characteristic length associated to the selected bandwidth

From this we can conclude that for a LOS distance above 8.23m, the MPC over the ground will start interfering with the LOS component. For a channel with 900MHz bandwidth, this value increases to 15.2m

Although the over the ground MPC is (in most cases) the shortest one, other MPCs can also be associated a minimum d_{LOS} distance above which the MPC will also interfere with the LOS signal. Once multiple MPC have reached this distance, they will interfere not only with the LOS signal but with each other as well. By changing the position of the tag very slightly, the MPC can appear or disappear and their interference can also drastically change.
Every localization requiring rangings with different anchors situated in very different spots, each anchor will be affected by different MPCs.

4.3 1^{st} experience - No MPC

A first set of measurements was performed in the UA2 lab. This experience serves as a reference for measurements without MPC interference as the area over which the measurements are performed is small enough and there are no obstacles (except the floor).

The figure below shows the real and estimated positions of the tag once on a graph including the anchors (left), and once zoomed in on the positions of the tag only (right). The x and y coordinates along the axes are expressed in meters. Each figure in this chapter follows the same structure

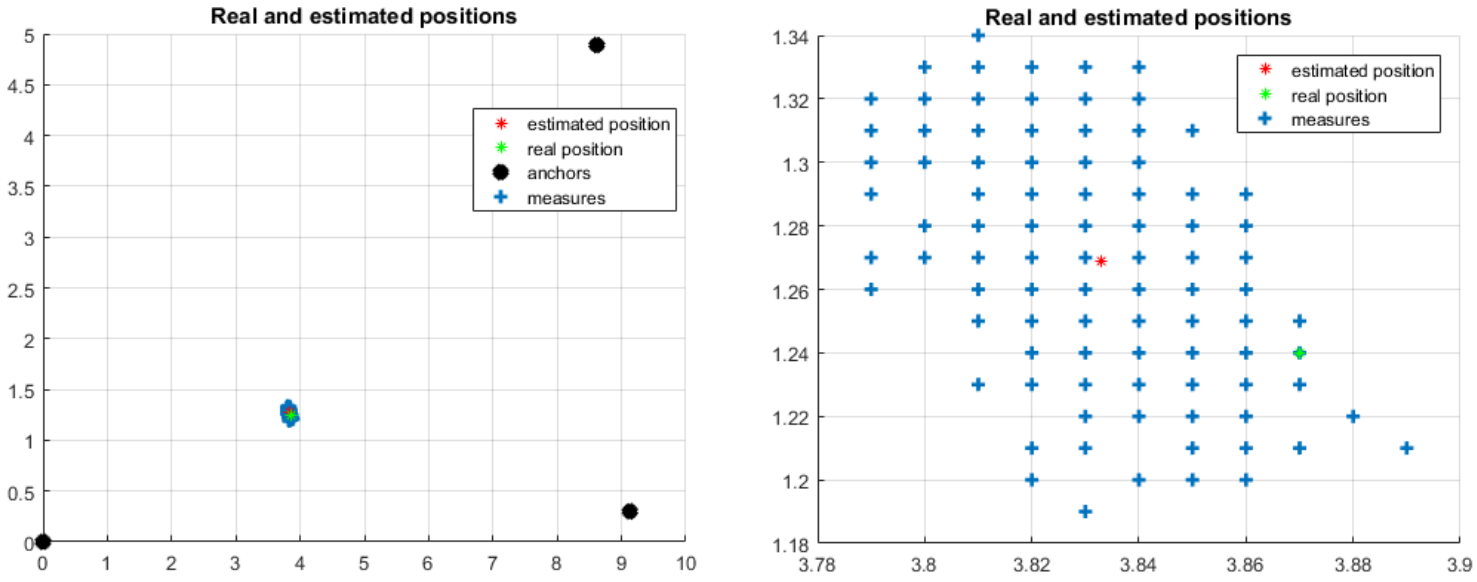

Figure 4.3.1: Position inside anchor triangle

The error on the position is in line with the errors on the single distance error presented in section 3.3.

- error between estimated and real positions: 0.0469 m
- maximum error: 0.1166 m

The distances to each of the anchors are under the 8.23m threshold for MPC interference.

Anchor	real distance(m)	measured distance(m)	error(m)
1	4.0638	4.0717	0.0079
2	5.3433	5.4102	0.0669
3	5.9864	6.0211	0.0347

Table 4.2: Ranging distances

A second measurement was performed in the same conditions, with the only change being the position of the tag which was placed further away from the center of the triangle defined by the anchors. Intuitively, this can be understood by

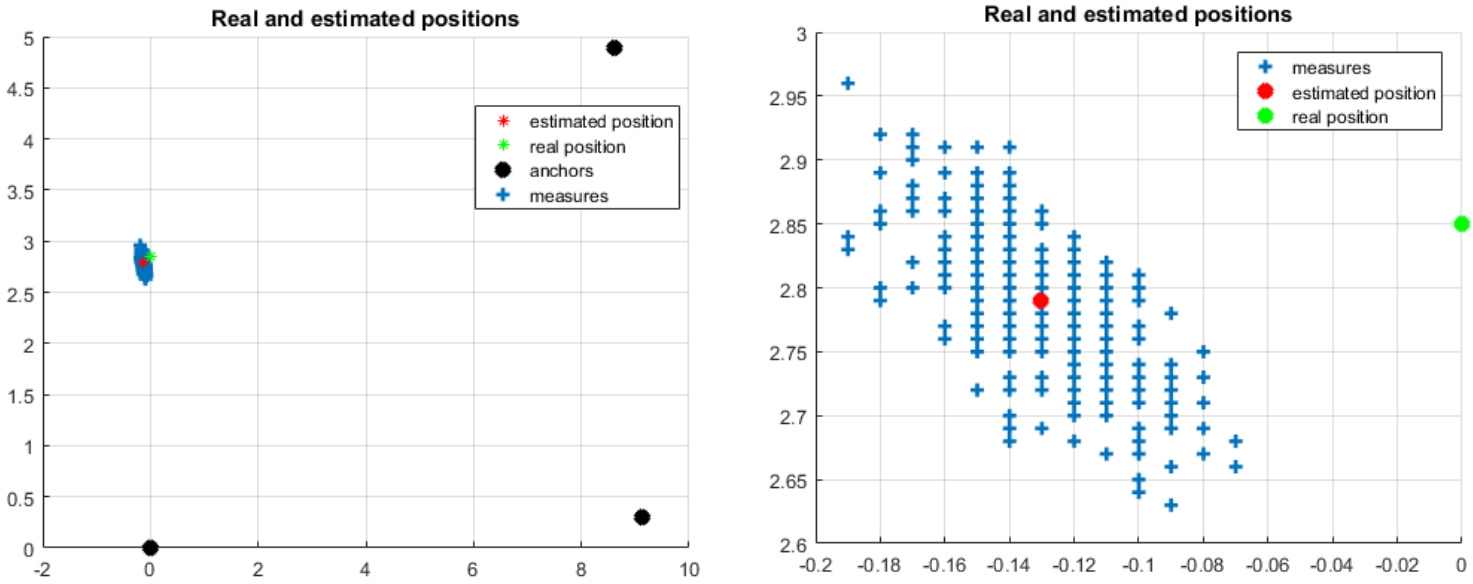

Figure 4.3.2: Position outside anchor triangle

The error on the position was increased by 10 cm compared to the previous experience, considering nothing but the position of the tag changed.

- error between estimated and real positions: 0.1435 m
- maximum error: 0.2377 m

Anchor	real distance(m)	measured distance(m)	error(m)
1	2.85	2.7930	0.0570
2	9.4794	9.5894	0.1099
3	8.8532	8.9941	0.1409

Table 4.3: Ranging distances

The conclusion to draw from these experiments is that the accuracy of the localization decreases when the tag leaves the triangle defined by the anchors, or more generally when the anchor gets away from the center of the triangle. Intuitively this can be understood by remembering figure 2.4.1. When the anchor gets further away from (at least) 2 of the anchors, the appear closer together and their LOPs start to superpose. A small error in the measurement of the distance will then lead to a large difference in the point of intersection of the LOPs.

4.4 Parking - MPC

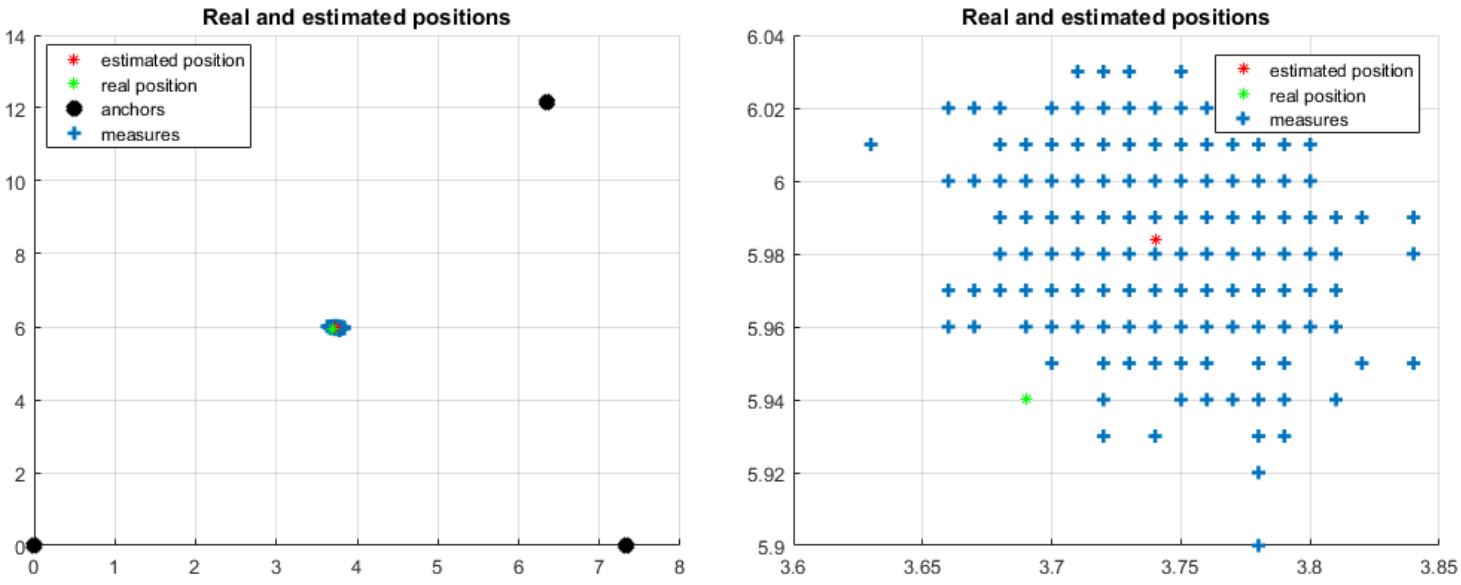

Figure 4.4.1: Parking inside triangle - std@110kbps

- error between estimated and real positions: 0.0667 m
- maximum error: 0.1581 m

Anchor	real distance(m)	measured distance(m)	error(m)
1	6.9928	7.1873	0.1945
2	6.966	7.1101	0.1435
3	6.7649	6.8426	0.0777

Table 4.4: Ranging distances

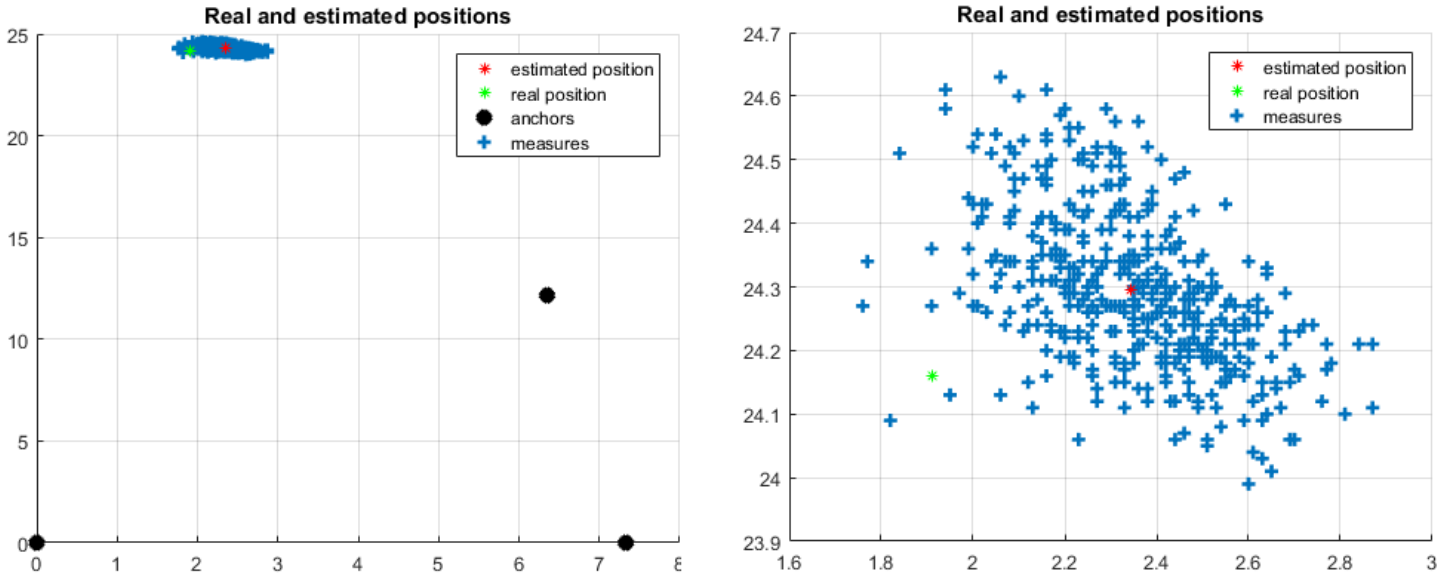

Figure 4.4.2: Position outside triangle std@110kbps

- error between estimated and real positions: 0.4526 m
- maximum error: 0.9613 m

Channel 7 has the same center frequency than channel 5 but has a bandwidth of 900MHz compared to the 500MHz for channel 5. The other parameters will be kept the same[1]

[1]except the preamble code which is channel dependent but doesn't influence the quality of the communication

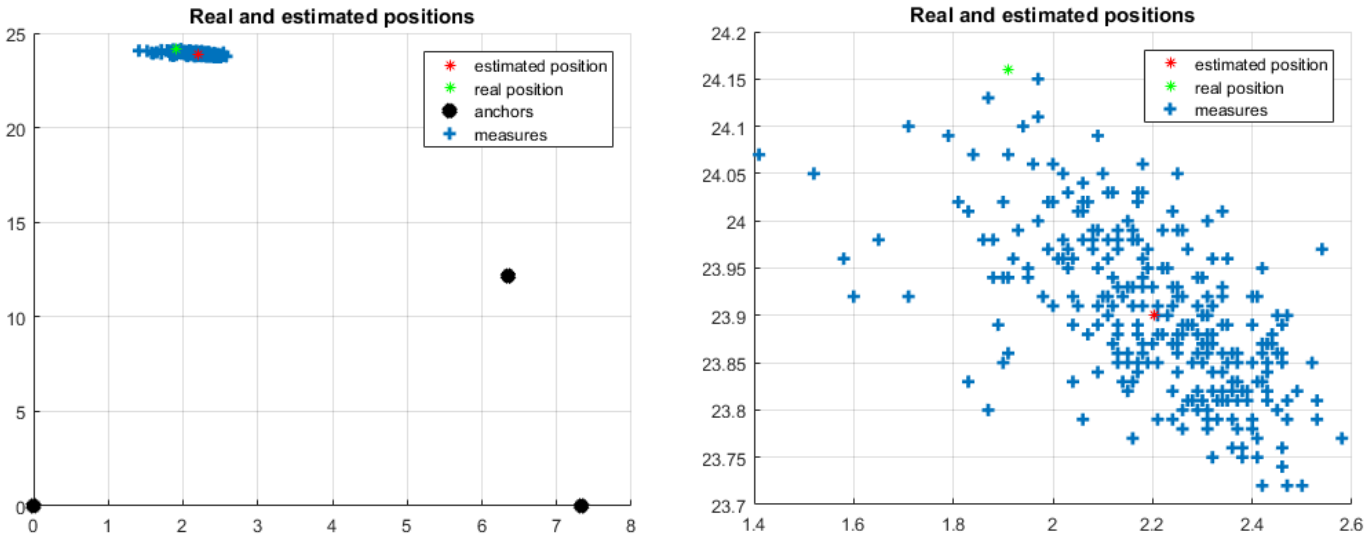

Figure 4.4.3: Position outside triangle - channel 7@110kbps

- error between estimated and real positions: 0.3906 m
- maximum error: 0.7752 m

The larger bandwidth of channel 7 improves the accuracy of the localization by 6cm.

4.5 Conclusion

In this chapter the first localization experiences were performed to study the accuracy of the localization algorithm and the influence of MPC on the localization. The communication performed with a larger bandwidth of 900MHz proved to give improved results compared to its 500MHz counterpart.

Chapter 5

Tracking

5.1 Introduction

This last chapter will display the behavior of the RTLS when it is tasked to track the position of the tag over time while the tag is moving. The first part will focus on environments with less constraints, that is when the environment is less prone to induce MPC affecting the LOS communication.

5.2 UA2

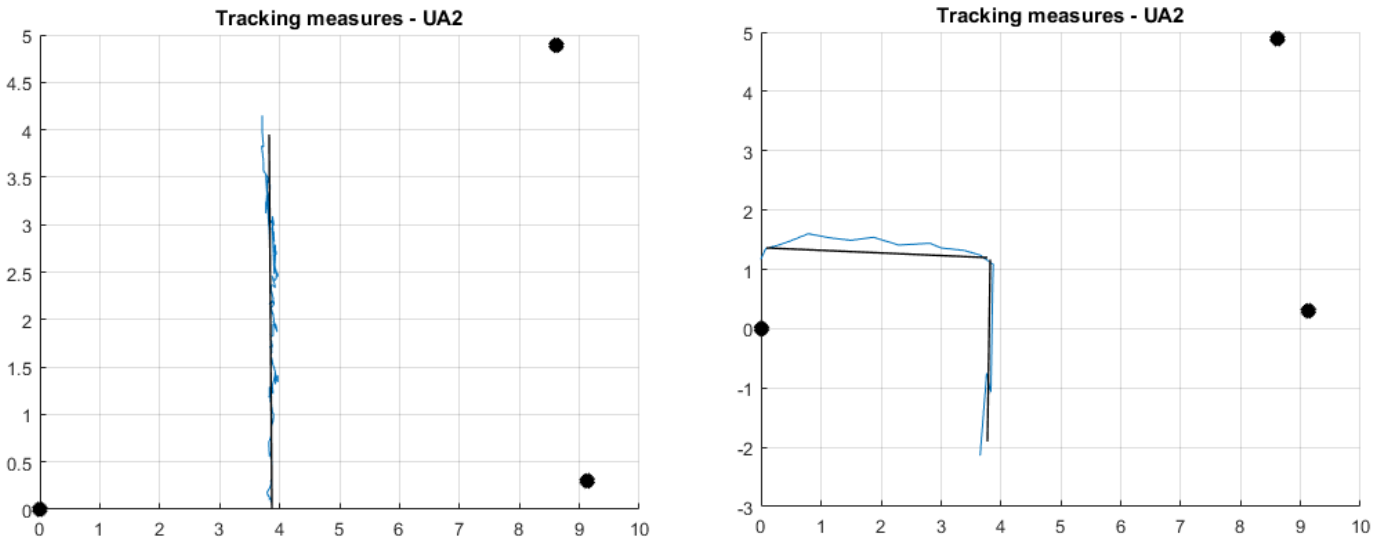

Figure 5.2.1: UA2 tracking trajectories

The measurement proceeded as planned, with a small deviation in the experiment on the right but nothing worth mentioning.

5.3 parking

Tracking tests were also realized in the underground parking described in section 4.1.1. The anchors were placed on the camera bases at a height of 1.6m as before, but the tag was this time carried in a moving car. An unintended consequence of this was that due to the metal chassis of the car, *the MPC over the ground could be blocked for certain positions of the car* when the anchors are behind the car. Other MPCs were not affected by this.

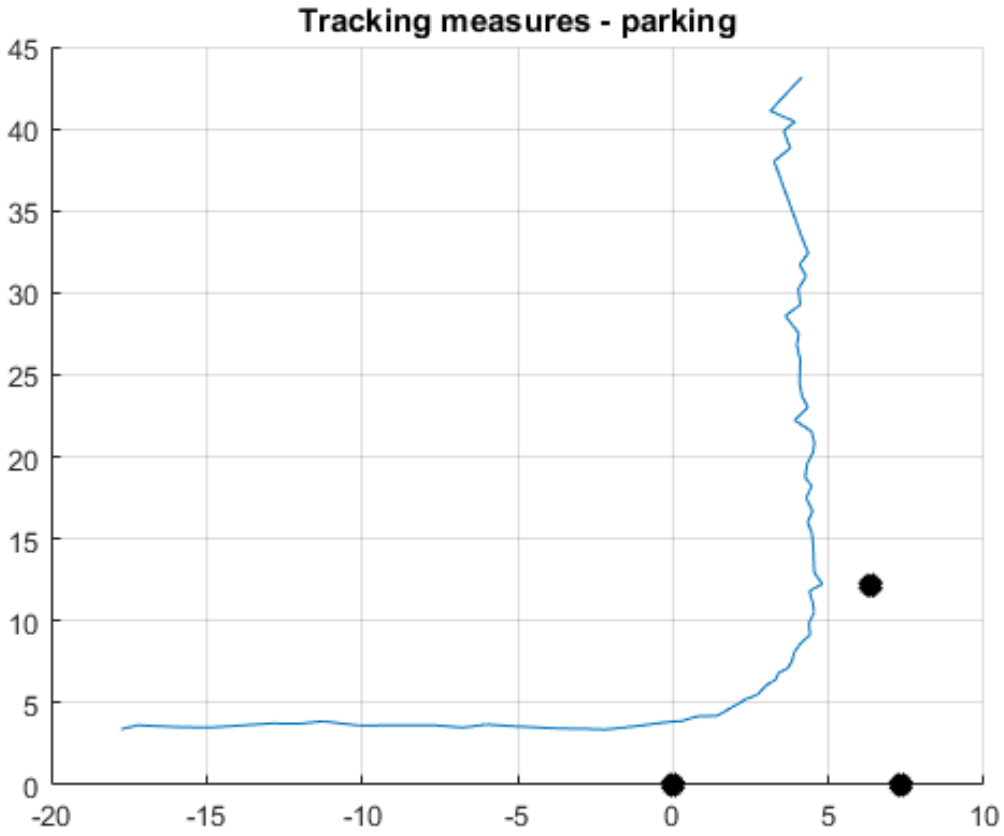

Figure 5.3.1: turn in parking

The first measurement performed is very interesting. The car starts at the point closest to the origin on the graphic, which corresponds to the elevated area of the parking. This tilt provides a protection to the MPC over the ground. The geometry of the ceiling also provides obstacles to other MPC components such that in this first zone, the interference is minimal, explaining the smoothness of the curve.

In the second part of the trajectory however this is not the case anymore. The MPC over the ground is present and periodically (since the columns do not form a continuous surface) MPCs from the columns also interfere with the LOS component.

The last 2 measurements below show measurements where the MPC over the ground is by times obstructed as the car drives by the anchors. The most left point of the position measurements on the left figure shows the point where the car was parked between 2 columns (before losing the signal), and then reversed.

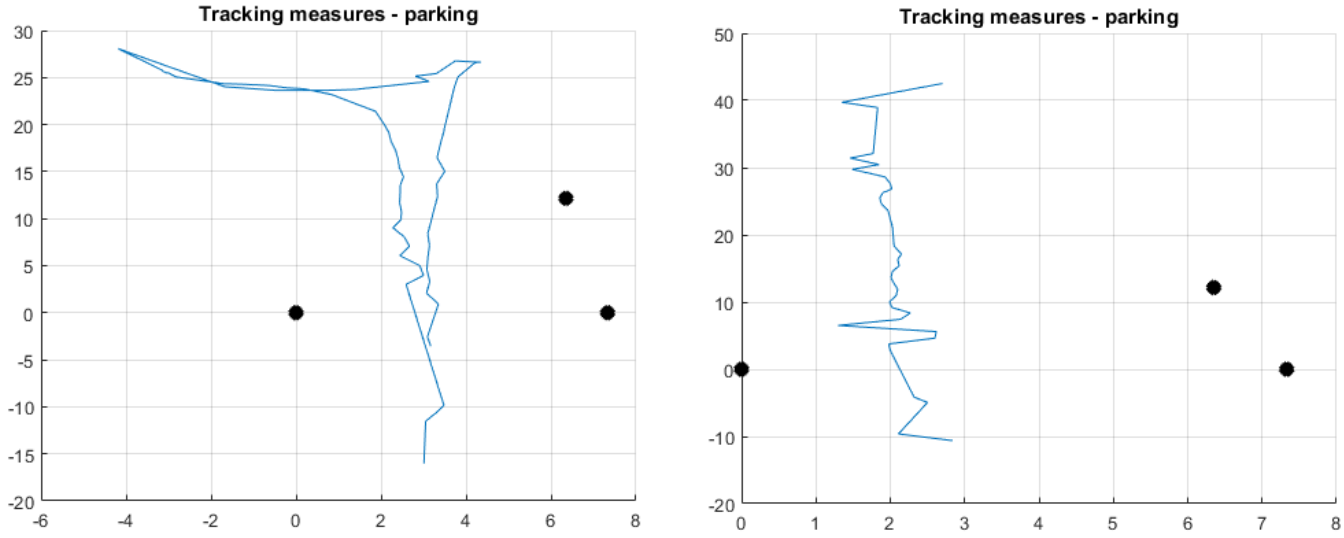

Figure 5.3.2: moving car and parking

For the figure on the left, the car was driven in a straight line and parked in a parking spot before turning around and doing the traject in the opposite direction. For the figure on the right, the car followed a simple straight line.

5.4 Conclusion

In the rare case where the underground environment geometry cancels the MPC by itself, we fall back on the outdoor case with close to no error. However this is generally not the case as many sources of interference exist and their multipath will affect the LOS once the MPC's length is close enough to that of the LOS. The fact that the car itself interfered with the ranging by blocking the over the ground MPC is the perfect illustration of this fact.

Chapter 6

Conclusion and future work

This project has been decomposed in 3 parts. The first part was to choose the ranging method of the RTLS, chosen to be the Symmetric Double Sided Two Way Ranging (SDS-TWR). The second part consisted in obtaining a functioning RTLS in outdoor conditions. The third part was to adapt this RTLS to perform in underground tunnels. This brought additional constraining factors as the outdoor version implemented was not able to perform in this environment.

Underground tunnels represent a big difficulty to overcome when designing an RTLS. At small distances or in outdoor environments, when no interference came into play, no problem was encountered. However during the transition to underground tunnels, the maximum coverable distance of the RTLS dropped from around 100m to 20m. Different parameters were changed to adapt to this new environment. In particular, positioning the tag and anchors as much as possible above the floor proved to be a simple yet very effective fix. Combined with a lowering of the data rate, the RTLS was re-established to cover the total distance available of 70m.

Compared to commercially available RTLS [13, 14, 15], this RTLS has a longer range. However the price to pay for this was a decrease of the frequency of position updates: while the commercial systems allow for update rates of around 100Hz, this one cannot reach more than 5 Hz.

Several improvements could be made to this RTLS. The most important improvement would be to allow the tag to select which anchors it ranges with. Although the current system allows an arbitrary amount of anchors (with the trade-offs that come with the increase), it doesn't allow the tag to select which anchors it performs ranging operations with. This should be implemented to allow the tag to move along a long distance (as is the case for train or metro systems) by placing tags regularly on its way.
Next in line would be to improve the update frequency which sits quite low at about 5Hz. Although this is sufficient when driving in a car at a moderate speed, it seems low for a real train or metro systems. These updated frequency measurements could then be followed by the implementation of Kalman filters to improve the tracking.
An interesting idea to explore would be to evaluate if 2 anchors instead of 3 could be sufficient for the desired application. Indeed, since metros and trains move on a predetermined track, it would be interesting to see if this additional information could replace the 3^{rd} anchor.

To conclude, the RTLS discussed in this work is suitable as a base for the desired application of tracking a vehicle in underground tunnels with high accuracy using UWB ranging. However it lacks a dynamic way of updating the anchors used for ranging to be able to track a vehicle over long distance that cannot be covered by a single anchor.

Appendix A

References

Bibliography

[1] Poszyx. *Solutions for asset tracking*. https://www.pozyx.io/applications/asset-tracking

[2] Guo, Kexin & Qiu, Zhirong & Miao, Cunxiao & Zaini, Abdul & Chen, Chun-Lin & Meng, Wei & Xie, Lihua. (2016). Ultra-Wideband-Based Localization for Quadcopter Navigation. Unmanned Systems. 1-12. 10.1142/S2301385016400033.

[3] Beams. *Master thesis subject proposal*. http://beams.ulb.ac.be/student-projects/master-thesis/beams-ee-fq-vehicle-localization-in-underground-tunnels-using-ultra-w

[4] Sewio Networks. *UWB Technology comparison*. https://rtlsuwb.com/#uwb

[5] Rafael Saraiva Campos, Lisandro Lovisolo. *RF Positioning. Fundamentals, Applications, and Tools*

[6] Decawave. *ScenSor Designing the first commercial IEEE 802.15.4a chip* https://www.decawave.com/sites/default/files/resources/ieee_eilat_nov_2012_slide_presentation.pdf

[7] http://www.sgo.fi/Greenland2011/l/08_Semeter_Radar_SP.pdf

[8] ScienceDirect. *Ultra-Wideband*. https://www.sciencedirect.com/topics/engineering/ultra-wideband

[9] IEEE Computer Society. *IEEE Std 802.15.4-2011* http://ecee.colorado.edu/~liue/teaching/comm_standards/2015S_zigbee/802.15.4-2011.pdf

[10] . Faranak Nekoogar. *Ultra-Wideband Communications: Fundamentals and Applications*, Chapter 1. Published Aug 31, 2005 by Prentice Hall. Part of the Prentice Hall Communications Engineering and Emerging Technologies Series from Ted Rappaport series. https://pdfs.semanticscholar.org/be5a/8190e3a1c6aab1d0d3eb03ab482b61b363f4.pdf

[11] Decawave. *APS011 Application note: sources of error in DW1000 based two-way ranging (TWR) schemes*.https://www.decawave.com/sites/default/files/resources/aps011_sources_of_error_in_twr.pdf

[12] Philippe Dedoncker. ELEC-H415 Communication channels.

[13] Poszyx. *Developer tag*. https://www.pozyx.io/shop/product/developer-tag-68

[14] Sewio. *RTLS System Overview*.

[15] Locatify. *Precise Indoor Positioning is finally here thanks to Ultra-wideband RTLS*. https://locatify.com/blog/in-practice-precise-indoor-location-detection-with-uwb-ultra-wideband/ http://www.sewio.net/wp-content/uploads/productlist/RTLS_overview_datasheet_v0.1.pdf

[16] Decawave. *Product documentation and application notes for DWM1000* https://www.decawave.com/product-documentation/

[17] Decawave. *Introduction to Real Time Location Systems*

[18] European Global navigation Satellite Agency (GSA). *What is GNSS*. https://www.gsa.europa.eu/european-gnss/what-gnss

[19] Fluke corporation. Fluke 411D user manual https://www.instrumart.com/assets/411D-manual.pdf

[20] Y. Zhou, "An efficient least-squares trilateration algorithm for mobile robot localization," 2009 IEEE/RSJ International Conference on Intelligent Robots and Systems, St. Louis, MO, 2009, pp. 3474-3479.http://vigir.missouri.edu/~gdesouza/Research/Conference_CDs/IEEE_IROS_2009/papers/0978.pdf

[21] Marko Bundalo. Electrical, Computer & Enery Engineering University of Colorado Boulder. *Ultra-WideBand*. http://ecee.colorado.edu/~ecen4242/marko/UWB/UWB/UWB.htm

[22] Jon Claerbout, Stanford Exploration Project. http://sepwww.stanford.edu/sep/prof/pvi/rand/paper_html/node2.html

[23] Pedro Aguiar, Institute for systems and robotics Lisbao. http://users.isr.ist.utl.pt/~aguiar/Notes_Chapter5.pdf

[24] Sparkfun. *Installing the ESP8266 Arduino Addon*. https://learn.sparkfun.com/tutorials/esp8266-thing-hookup-guide/installing-the-esp8266-arduino-addon

[25] Maxim Integrated. *Definition for Ultra-Wideband* https://www.maximintegrated.com/en/glossary/definitions.mvp/term/Ultra-Wideband/gpk/987

[26] Adafruit. *Adafruit Feather HUZZAH ESP8266* https://cdn-learn.adafruit.com/downloads/pdf/adafruit-feather-huzzah-esp8266.pdf

Appendix B

Using the system

B.1 How to send code to the board

Using Arduino IDE:

1. Download Arduino IDE https://www.arduino.cc/en/Main/Software
2. Add the library for esp8266 by going to *File* > *Preferences* > *Settings* > *Additional Boards Manager URLs*
   and adding the url :http://arduino.esp8266.com/stable/package_esp8266com_index.json
3. Navigate to *Tools* > *Boards* > *Boards Manager* and search for esp8266 and install the add-on.
4. Navigate to *Tools* > *Boards* and select *Adafruit Feather HUZZAH ESP8266* or *NodeMCU 1.0 (ESP-12E Module)*

Installing library in Arduino :

1. Navigate to *File* > *Preferences* to choose the location of the installed libraries
2. Navigate to *Sketch* > *Add .ZIP Library...* and choose the library. The zip has to contain a folder containing the files of the library.

Arduino can also be installed in a standalone folder that simply needs to be copied and pasted to the host machine(see https://www.arduino.cc/en/Guide/PortableIDE).

B.2 SPI communication

When using SPI functions, it is the SPI functions from the ESP library! And not from the default arduino one. The problem with the SPI functions inside the ESP library is that they do not correctly suspend the interrupts during the SPI communication (interrupts() and noInterrupts()). When an interrupt occurs during an SPI communication, the communication fails.

This problem doesn't show up until ranging attempts are performed since usage without interrupts does not reveal this problem.

Appendix C

Code

The complete code can be found at https://github.com/mgormez/vehicle_localization.

Each arduino sketch (*.ino) should be uploaded to an ESP. The difference between the different anchor sketches are simply the anchor number that is set and used to identify the anchor.

The main program loop is in the file uC.cpp, where one can find the ranging, distance and position implementations.
The files sensor.cpp, receiver.cpp and transmitter.cpp are use to translate the selected channel parameters to the appropriate values in the register of the dwm1000.

Appendix D

Trilateration in 2D plane

The error to minimize is given by

$$S(p_0) = \sum_{i=1}^{N}((p_i - p_0)^T(p_i - p_0) - r_i^2)^2$$

Solving this problem is equivalent to finding p_0 such that

$$\frac{\partial S(p_0)}{\partial p_0} = a + Bp_0 + [2p_0p_0^T] + (p_0^Tp_0)I]c - p_0p_0^Tp_0 = 0 \tag{D.1}$$

where

$$p_0 = \begin{pmatrix} x_0 \\ y_0 \end{pmatrix}$$
$$I = identity\ matrix$$
$$a = \frac{1}{N}\sum_{i=1}^{N}[p_ip_i^Tp_i - r_i2p_i]$$
$$B = \frac{1}{N}\sum_{i=1}^{N}[-2p_ip_i^T - (p_ip_i^T)Ir_i2I]$$
$$c = \frac{1}{N}\sum_{i=1}^{N}p_i$$

To simplify equation D.1, we introduce a linear transform

$$p_0 = q + c$$

Which gives an equation without quadratic dependence in q

$$(a + Bc + 2cc^Tc) + \{Bq + [2cc^T + (c^Tc)I]q\} - qq^Tq = 0$$

We then write

$$f = a + Bc + 2cc^Tc$$
$$H = -\frac{2}{N}\sum_{i=1}^{N}p_ip_i^T + 2cc^T$$
$$q = -H^{-1}f$$

and compute p_0

$$p_0 = q + c$$